1974-09

Hybrid mode analysis of microstrip on dielectric and ferrite substrate

Tüfekcioglu, Ahmet Munir

Monterey, California. Naval Postgraduate School

HYBRID MODE ANALYSIS OF MICROSTRIP ON DIELECTRIC AND FERRITE SUBSTRATE

Ahmet Münir Tüfekçioğlu

NAVAL POSTGRADUATE SCHOOL
Monterey, California

THESIS

HYBRID MODE ANALYSIS OF MICROSTRIP
ON
DIELECTRIC AND FERRITE SUBSTRATE

Ahmet Münir Tüfekçioğlu

September 1974

Thesis Advisor: J. B. Knorr

REPORT DOCUMENTATION PAGE

READ INSTRUCTIONS BEFORE COMPLETING FORM

1. REPORT NUMBER

2. GOVT ACCESSION NO.

3. RECIPIENT'S CATALOG NUMBER

4. TITLE (and Subtitle)
Hybrid Mode Analysis of Microstrip on Dielectric and Ferrite Substrate

5. TYPE OF REPORT & PERIOD COVERED
Electrical Engineer; September 1974

6. PERFORMING ORG. REPORT NUMBER

7. AUTHOR(s)
Ahmet Münir Tüfekçioḡlu

8. CONTRACT OR GRANT NUMBER(s)

9. PERFORMING ORGANIZATION NAME AND ADDRESS
Naval Postgraduate School
Monterey, California 93940

10. PROGRAM ELEMENT, PROJECT, TASK AREA & WORK UNIT NUMBERS

11. CONTROLLING OFFICE NAME AND ADDRESS
Naval Postgraduate School
Monterey, California 93940

12. REPORT DATE
September 1974

13. NUMBER OF PAGES
95

14. MONITORING AGENCY NAME & ADDRESS (if different from Controlling Office)
Naval Postgraduate School
Monterey, California 93940

15. SECURITY CLASS. (of this report)
Unclassified

15a. DECLASSIFICATION/DOWNGRADING SCHEDULE

16. DISTRIBUTION STATEMENT (of this Report)

Approved for public release; distribution unlimited.

17. DISTRIBUTION STATEMENT (of the abstract entered in Block 20, if different from Report)

18. SUPPLEMENTARY NOTES

19. KEY WORDS (Continue on reverse side if necessary and identify by block number)

Microstrip
Spectral Domain Transform
Method of Moments

20. ABSTRACT (Continue on reverse side if necessary and identify by block number)

A hybrid mode analysis of microstrip on a dielectric substrate is presented. A numerical solution for wavelength and characteristic impedance of single and coupled, balanced strips is obtained. Line parameters are shown to be very frequency dependent but in agreement with the quasi-static results of other investigators in the low frequency limit.

Block #20 Continued.

The extension of this technique to perturbation analysis of microstrip on ferrite is also described. A numerical solution for the propagation constant is obtained.

Hybrid Mode Analysis of Microstrip

on

Dielectric and Ferrite Substrate

by

Ahmet Münir Tüfekçioğlu
Lieutenant (jg), Turkish Navy
B.S.E.E., Naval Postgraduate School, 1973
M.S.E.E., Naval Postgraduate School, 1973

Submitted in partial fulfillment of the
requirements for the degree of

ELECTRICAL ENGINEER

from the

NAVAL POSTGRADUATE SCHOOL
September 1974

ABSTRACT

A hybrid mode analysis of microstrip on a dielectric substrate is presented. A numerical solution for wavelength and characteristic impedance of single and coupled, balanced strips is obtained. Line parameters are shown to be very frequency dependent but in agreement with the quasi-static results of other investigators in the low frequency limit.

The extension of this technique to perturbation analysis of microstrip on ferrite is also described. A numerical solution for the propagation constant is obtained.

TABLE OF CONTENTS

LIST OF TABLES

TABLE

LIST OF FIGURES

Figure

Figure

ACKNOWLEDGEMENT

The author gratefully expresses his gratitude to Professor Jeffrey B. Knorr for his considerable help and guidance during this study and his patience in editing this thesis.

Also of great help has been the encouragement in this work of my wife, Adalet, who carefully and patiently typed the first draft.

I. INTRODUCTION

The analysis of microstrip is of great importance as this type of transmission line has found wide use due to its compatibility with microwave integrated circuitry. The open microstrip transmission line has been predominant because it can be etched or deposited easily on the substrate.

The early analytic work on microstrip lines has been based on a proposed TEM mode of propagation which is, in essense, a static approximation to a dynamic system. For sufficiently low frequencies the quasi-static theory can be employed to obtain the characteristics of microstrip lines. When the wavelength in a microstrip line becomes comparable to transverse dimensions of the line the deviation from quasi-static behavior becomes significant and high order modes of propagation become possible.

In this present work a Spectral Domain transform method is applied for calculating the frequency dependent characteristics of single and coupled microstrip transmission lines. Effects of geometry on the dispersion and characteristic impedance have been analyzed.

Figures 1 and 2 show the geometry of the microstrip line. The strip conductor is assumed to be infinitely thin and perfectly conducting and the ground plane and dielectric or ferrite substrate are assumed to be infinite in extent.

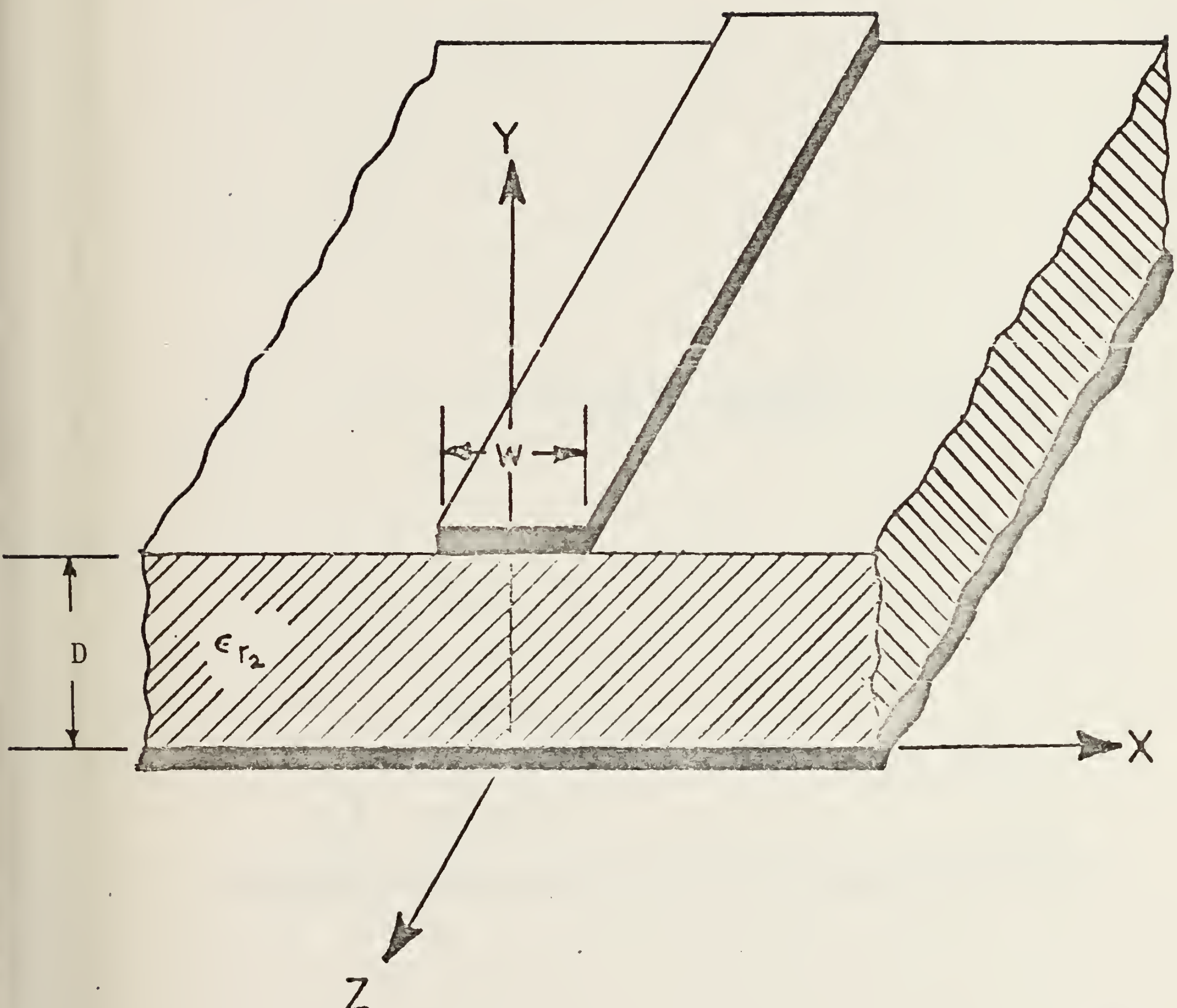

Figure 1. Three Dimensional Microstrip Transmission Line.

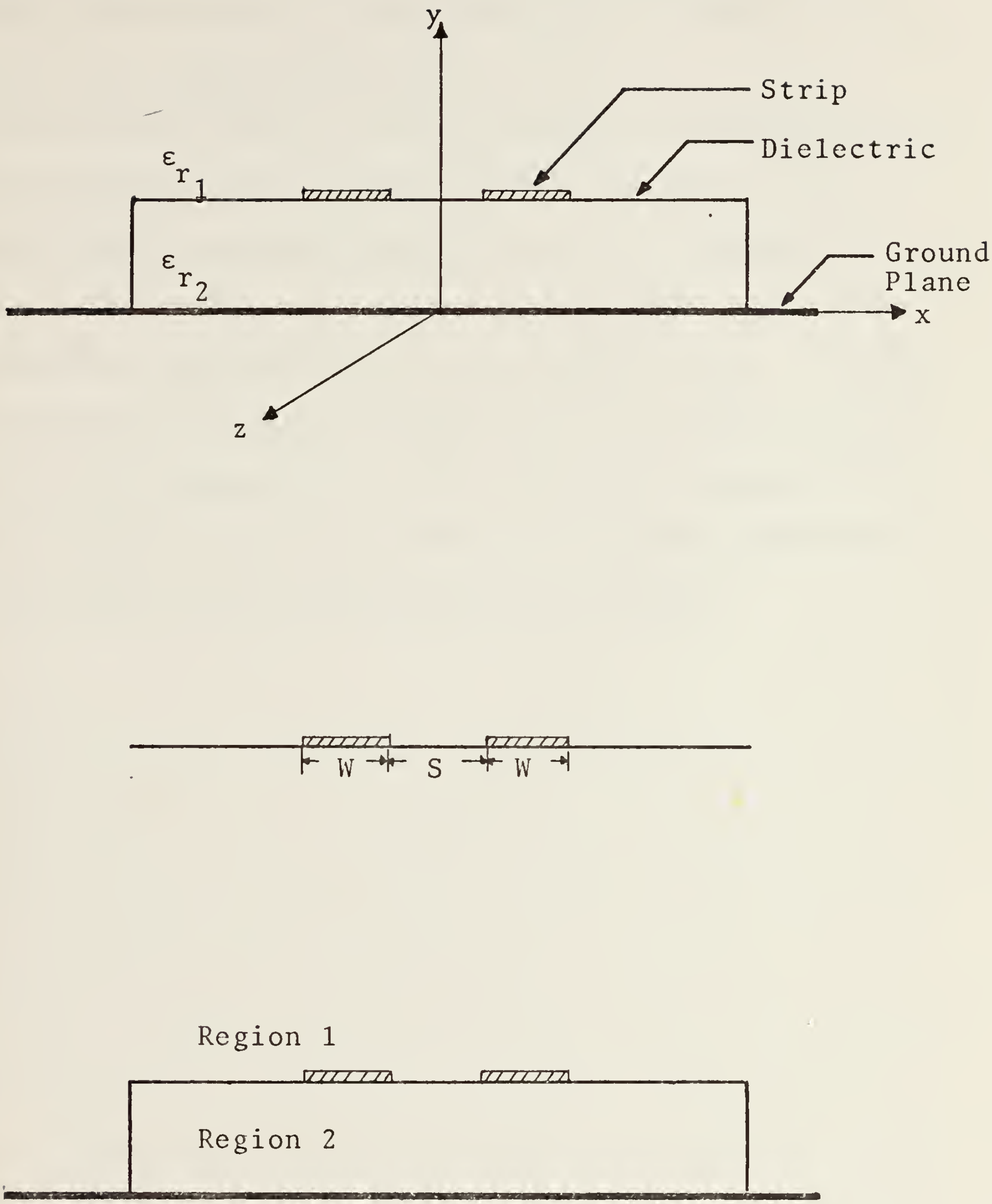

Figure 2. Coupled Microstrip and Regions.

It is assumed initially that the substrate material is lossless and isotropic. Lossy anisotropic substrates are treated later using perturbation theory.

The Spectral Domain transform method was suggested by Itoh and Mittra, [Ref. 6] and yields a solution to the Boundary value problem of microstrip via the method of moments. The method was used by Itoh and Mittra to find the dispersion characteristics of a single strip. In this work the method has been extended to cover dispersion and characteristic impedance of both single and coupled microstrips. The case of a microstrip on a ferrite substrate has also been solved using perturbation theory.

II. DISPERSION CHARACTERISTICS ON DIELECTRIC SUBSTRATE

A. FIELD AND BOUNDARY CONDITIONS

Let the following electric and magnetic fields exist and propagate in the z-direction as justified by the Hertzian Vector Potential functions described in Appendix A.

$$E_z = k_c^2 \phi^e e^{\gamma z} \tag{1}$$

$$H_z = k_c^2 \phi^e e^{\gamma z} \tag{2}$$

where γ is the Propagation constant. For the lossless substrate material

$$\gamma = j\beta .$$

From the field expressions in equation (1) and (2) all other components of electric and magnetic field can be derived from Maxwell's curl equations, as shown in Appendix B and leads to the following equations.

$$E_x = \left(\gamma \frac{\partial \phi^e}{\partial x} - j\omega\mu \frac{\partial \phi^h}{\partial y}\right) e^{\gamma z} \tag{3}$$

$$H_x = \left(\gamma \frac{\partial \phi^h}{\partial x} + j\omega\varepsilon \frac{\partial \phi^e}{\partial y}\right) e^{\gamma z} \tag{4}$$

$$E_y = \left(\gamma \frac{\partial \phi^e}{\partial y} + j\omega\mu \frac{\partial \phi^h}{\partial x}\right) e^{\gamma z} \tag{5}$$

$$H_y = \left(\gamma \frac{\partial \phi^h}{\partial y} - j\omega\varepsilon \frac{\partial \phi^e}{\partial x}\right) e^{\gamma z} . \tag{6}$$

Applying boundary conditions at the interface between region 2 and the ground plane, tangential electric fields must be zero, so it follows that at $y = 0$,

$$E_{z_2}(x,0,z) = 0 \tag{7}$$

$$E_{x_2}(x,0,z) = 0. \tag{8}$$

Also at the interface between regions 1 and 2, tangential electric fields must be continuous:

At $y = D$,

$$E_{z_1}(x,D,z) = E_{z_2}(x,D,z) \tag{9}$$

$$E_{x_1}(x,D,z) = E_{x_2}(x,D,z). \tag{10}$$

Also the electric fields will exist only in the dielectric part of the interface and can be expressed as,

$$E_{z_1}(x,D,z) = \begin{cases} 0 & \text{on strip} \\ e_z(x)e^{\gamma z} & \text{elsewhere} \end{cases} \tag{11}$$

$$E_{x_1}(x,D,z) = \begin{cases} 0 & \text{on strip} \\ e_x(x)e^{\gamma z} & \text{elsewhere} \end{cases} \tag{12}$$

Similarly, tangential magnetic fields must be discontinuous by corresponding surface current densities

$$H_{z_1}(x,D,z) - H_{z_2}(x,D,z) = \begin{cases} J_x(x)e^{\gamma z} & \text{on strip} \\ 0 & \text{elsewhere.} \end{cases} \tag{13}$$

$$H_{x_1}(x,D,z) - H_{x_2}(x,D,z) = \begin{cases} J_z(x)\, e^{\gamma z} & \text{on strip} \\ 0 & \text{elsewhere.} \end{cases} \tag{14}$$

Substituting the field expressions of equation (1) through (6) into the boundary condition expressions of equations (7) through (14), one obtains

$$k_{c_2}^2 \phi_2^e(x,0) = 0 \tag{15}$$

$$\gamma \frac{\partial \phi_2^e}{\partial x}(x,0) - j\omega\mu_2 \frac{\partial \phi_2^h}{\partial y}(x,0) = 0 \tag{16}$$

$$k_{c_1}^2 \phi_1^e(x,D) = k_{c_2}^2 \phi^e(x,D) \tag{17}$$

$$\gamma \frac{\partial \phi_1^e(x,D)}{\partial x} - j\omega\mu_1 \frac{\partial \phi_1^h(x,D)}{\partial y} = \gamma \frac{\partial \phi_2^e(x,D)}{\partial x} - j\omega\mu_2 \frac{\partial \phi_2^h(x,D)}{\partial y} \tag{18}$$

$$k_{c_1}^2 \phi_1^e(x,D) = \begin{cases} 0 & \text{on strip} \\ e_z(x) & \text{elsewhere} \end{cases} \tag{19}$$

$$\gamma \frac{\partial \phi_1^e(x,D)}{\partial x} - j\omega\mu_1 \frac{\partial \phi_1^h(x,D)}{\partial y} = \begin{cases} 0 & \text{on strip} \\ e_x(x) & \text{elsewhere} \end{cases} \tag{20}$$

$$k_{c_1}^2 \phi_1^h(x,D) - k_{c_2}^2 \phi_2^h(x,D) = \begin{cases} J_x(x) & \text{on strip} \\ 0 & \text{elsewhere} \end{cases} \tag{21}$$

$$\left(\gamma\frac{\partial\phi_1^h(x,D)}{\partial x} + j\omega\varepsilon_1 \frac{\partial\phi_1^e(x,D)}{\partial y}\right)$$

$$- \left(\gamma\frac{\partial\phi_2^h(x,D)}{\partial x} + j\omega\varepsilon_2 \frac{\partial\phi_2^e(x,D)}{\partial y}\right) = \begin{cases} J_z(x) & \text{on strip} \\ 0 & \text{elsewhere} \end{cases} \tag{22}$$

B. SPECTRAL DOMAIN TRANSFORM

All potential functions must satisfy the following relation:

$$\nabla_t^2\phi + k_c^2\,\phi = 0 \tag{23}$$

where

$$k_c^2 = \gamma^2 + k^2 = k^2 - \beta^2. \tag{24}$$

One introduces the Fourier transform to the α-domain, as suggested by Itoh and Mittra:

$$\Phi_i(\alpha,y) = \int_{-\infty}^{+\infty} \phi_i(x,y)e^{j\alpha x}dx \qquad i = 1,2,3... \tag{25}$$

Thus, the transform of equation (23) becomes

$$F_x\left[\frac{\partial^2\phi}{\partial x^2}\right] + F_x\left[\frac{\partial^2\phi}{\partial y^2}\right] + k_c^2\,F_x[\phi] = 0 \tag{26}$$

$$(j\alpha)^2\,F_x[\phi(x,y)] + \frac{\partial^2}{\partial y^2}F_x[\phi(x,y)] + k_c^2\,F_x[\phi] = 0 \tag{27}$$

where

$$F_x\left[\frac{\partial\phi(x,y)}{\partial x}\right] = -j\alpha\,F_x[\phi(x,y)] \tag{28}$$

has been applied.

Clearly, one can obtain α-domain representation of equation (23),

$$-\alpha^2 \Phi(\alpha,y) + \frac{\partial^2}{\partial y^2} \Phi(\alpha,y) + k_c^2 \Phi(\alpha,y) = 0 \qquad (29)$$

or

$$\frac{\partial^2 \Phi(\alpha,y)}{\partial y} = (\alpha^2 - k_c^2) \Phi(\alpha,y). \qquad (30)$$

Equation (30) should be analyzed carefully both for Region 1 and Region 2.

For Region 1, (free space propagation constant),

$$\gamma_1^2 = \alpha_1^2 - k_{c_1}^2 = \alpha^2 + \beta^2 - k_1^2 \qquad (31)$$

where

$$k_1 = \omega\sqrt{\mu_o \varepsilon_o} \quad \text{and} \quad \beta = \frac{2\pi}{\lambda'}$$

$$\gamma_1^2 = \alpha^2 + \left(\frac{2\pi}{\lambda}\right)^2 \left[\left(\frac{\lambda}{\lambda'}\right)^2 - 1\right]. \qquad (32)$$

λ' is the microstrip wavelength and is related to the free-space wavelength λ as

$$\lambda \geq \lambda' \geq \frac{\lambda}{\sqrt{\varepsilon_r}}. \qquad (33)$$

By substituting Equation (33) into (32) one can find lower and upper values for γ_1

$$\alpha^2 + (\varepsilon_{r_1} - 1)\left(\frac{2\pi}{\lambda}\right)^2 \geq \gamma_1^2 \geq \alpha^2. \qquad (34)$$

Therefore γ_1 is always a real quantity independent of the values of α.

Similarly for Region 2,

$$\gamma_2^2 = \alpha^2 - \left(\frac{2\pi}{\lambda} \right)^2 \left[\varepsilon_{r_2} - \left(\frac{\lambda}{\lambda'} \right)^2 \right] \tag{35}$$

so it is clear that γ_2 will be imaginary for

$$-\frac{2\pi}{\lambda}\sqrt{\varepsilon_{r_2} - \left(\frac{\lambda}{\lambda'} \right)^2} < \alpha < \frac{2\pi}{\lambda}\sqrt{\varepsilon_{r_2} - \left(\frac{\lambda}{\lambda'} \right)^2} \tag{36}$$

and will be real when α is in the range

$$-\infty<\alpha< -\frac{2\pi}{\lambda}\sqrt{\varepsilon_{r_2} - \left(\frac{\lambda}{\lambda'} \right)} \; ; \; \frac{2\pi}{\lambda}\sqrt{\varepsilon_{r_2} - \left(\frac{\lambda}{\lambda'} \right)^2} <\alpha<+\infty. \tag{37}$$

For Region 1, the field function differential equation solution is as follows:

$$\frac{\partial^2}{\partial y^2} \Phi_1(\alpha,y) = \gamma_1^2 \Phi(\alpha,y) = (\alpha^2 - k_{c_1}^2)\Phi_1(\alpha,y) \tag{38}$$

$$(s^2 - \gamma_1^2)\Phi_1(s) = 0. \tag{39}$$

Therefore,

$$\Phi_1(\alpha,y) = R_1(\alpha)e^{+\gamma_1 y} + R_2(\alpha)e^{-\gamma_1 y}. \tag{40}$$

Clearly, for infinite positive values of y, the field should vanish, or,

$$\lim_{y\to\infty} \Phi_1(\alpha,y) = 0 \tag{41}$$

then,

$$\Phi_1(\alpha,y) = R_2(\alpha)e^{-\gamma_1 y} = A(\alpha)e^{-\gamma_1 y} \tag{42}$$

where

$$A(\alpha) = R_2(\alpha).$$

Similarly for Region 2, there are two solutions, corresponding to the real or imaginary character of γ_2. The solution for γ_2 imaginary is

$$\Phi_2(\alpha,y) = B(\alpha)\mathrm{Sin}\gamma_2 y + C(\alpha)\mathrm{Cos}\gamma_2 y \tag{43}$$

where

$$\gamma_2 = j\gamma_2''$$

and for γ_2 real it is

$$\Phi_2(\alpha,y) = B(\alpha)\mathrm{Sinh}\gamma_2 y + C(\alpha)\mathrm{Cosh}\gamma_2 y. \tag{44}$$

Therefore, the transforms of ϕ_1^e, ϕ_1^h, ϕ_2^e, ϕ_2^h are given by

<u>Region 1</u>

$$\Phi_1^e(\alpha,y) = A^e(\alpha)e^{-\gamma_1(y-D)} \tag{45}$$

$$\Phi_1^h(\alpha,y) = A^h(\alpha)e^{-\gamma_1(y-D)} \tag{46}$$

<u>Region 2</u>

$$\Phi_2^e(\alpha,y) = \begin{cases} B_H^e(\alpha)\mathrm{Sinh}\gamma_2 y + C_H^e(\alpha)\mathrm{Cosh}\gamma_2 y, & \gamma_2 \text{ Real} \quad (47) \\ \\ jB_T^e(\alpha)\mathrm{Sin}\gamma_2'' y + C_T^e(\alpha)\mathrm{Cos}\gamma_2'' y, & \gamma_2 \text{ Imaginary} \quad (48) \end{cases}$$

$$\phi_2^h(\alpha,y) = \begin{cases} B_H^h(\alpha)\mathrm{Sinh}\gamma_2 y + C_H^h(\alpha)\mathrm{Cosh}\gamma_2 y, & \gamma_2 \text{ Real} \quad (49) \\ \\ jB_T^h(\alpha)\mathrm{Sin}\gamma_2'' y + C_H^h(\alpha)\mathrm{Cos}\gamma_2'' y, & \gamma_2 \text{ Imaginary} \quad (50) \end{cases}$$

where superscript (e) denotes the electric field case and (h) magnetic field case and where

$$\gamma_2'' = -j\gamma_2.$$

Spectral Domain representation of the boundary condition expressions can be obtained by taking the Fourier transform of the equations (7) through (14) with the following results:

$$k_{c_2}^2 \Phi_2^e(\alpha,0) = 0 \tag{51}$$

$$-j\alpha\gamma\Phi_2^e(\alpha,0) - j\omega\mu_2 \frac{\partial\Phi_2^h}{\partial y}(\alpha,0) = 0 \tag{52}$$

$$k_{c_1}^2 \Phi_1^e(\alpha,D) = k_{c_2}^2 \Phi_2^e(\alpha,D) \tag{53}$$

$$-j\alpha\gamma\Phi_1^e(\alpha,D) - j\omega\mu_1 \frac{\partial\Phi_1^h(\alpha,D)}{\partial y} = -j\alpha\gamma\Phi_2^e(\alpha,D) - j\omega\mu_2 \frac{\partial\Phi_2^h(\alpha,D)}{\partial y} \tag{54}$$

$$k_{c_1}^2 \Phi_1^e(\alpha,D) = E_z(\alpha) \tag{55}$$

$$-j\alpha\gamma\Phi_1^e(\alpha,D) - j\omega\mu_1 \frac{\partial\Phi_1^h}{\partial y}(\alpha,D) = E_x(\alpha) \tag{56}$$

$$k_{c_i}^2 \Phi_1^h(\alpha,D) - k_{c_2}^2 \Phi_2^h(\alpha,D) = J_x(\alpha) \tag{57}$$

$$-j\alpha\gamma\Phi_1^h(\alpha,D) + j\omega\varepsilon_1 \frac{\partial\Phi_1^e(\alpha,D)}{\partial y} + j\alpha\gamma\Phi_2^h(\alpha,D) - j\omega\varepsilon_2 \frac{\partial\Phi_2^e(\alpha,D)}{\partial y} = J_z(\alpha). \tag{58}$$

Where the derivative transform pair

$$F\left[\frac{\partial\phi(x,y)}{\partial x}\right] = -j\,\alpha\Phi(\alpha,y)$$

has been applied.

By substituting the Field expressions for real (hyperbolic case) and the imaginary (trigonometric case) values of γ_2 into the transformed equations (51) through (58), the following equations are obtained.

Hyperbolic Case:

$$k_{c_2}^2 C_H^e(\alpha) = 0 \tag{59}$$

$$-j[\alpha\gamma C_H^e(\alpha) + \omega\mu_2\gamma_2 B_H^h(\alpha)] = 0 \tag{60}$$

$$k_{c_1}^2 A^e(\alpha) = k_{c_2}^2 [C_H^e(\alpha)\operatorname{Cosh}\gamma_2 D + B_H^e(\alpha)\operatorname{Sinh}\gamma_2 D] \tag{61}$$

$$\begin{aligned} -j(\alpha\gamma A^e(\alpha) - \omega\mu_1\gamma_1 A^h(\alpha)) = &- j\alpha\gamma[B_H^e(\alpha)\operatorname{Sinh}\gamma_2 D + \\ &C_H^e(\alpha)\operatorname{Cosh}\gamma_2 D] - j\omega\mu_2\gamma_2[B_H^h(\alpha)\operatorname{Cosh}\gamma_2 D + C_H^h(\alpha)\operatorname{Sinh}\gamma_2 D] \end{aligned} \tag{62}$$

$$k_{c_1}^2 A^e(\alpha) = E_z(\alpha) \tag{63}$$

$$-j(\alpha\gamma A^e(\alpha) - \omega\mu_1\gamma_1 A^h(\alpha)) = E_x(\alpha) \tag{64}$$

$$k_{c_1}^2 A^h(\alpha) - k_{c_2}^2 [B_H^h(\alpha)\operatorname{Sinh}\gamma_2 D + C_H^h(\alpha)\operatorname{Cosh}\gamma_2 D] = J_x(\alpha) \tag{65}$$

$$\begin{aligned} -j(\alpha\gamma A^h(\alpha) + \omega\varepsilon_1\gamma_1 A^e(\alpha)) &+ j\alpha\gamma[B_H^h(\alpha)\operatorname{Sinh}\gamma_2 D + C_H^h(\alpha)\operatorname{Cosh}\gamma_2 D] \\ &-j\omega\varepsilon_2\gamma_2[B_H^e(\alpha)\operatorname{Cosh}\gamma_2 D + C_H^e(\alpha)\operatorname{Sinh}\gamma_2 D] = J_z(\alpha). \end{aligned} \tag{66}$$

Similarly for imaginary values of γ_2 by making the substitutions

$$\gamma_2 = j\gamma_2''$$

$$\operatorname{Sinh}\gamma_2 D = j\operatorname{Sin}\gamma_2'' D \tag{67}$$

$$\text{Cosh}\gamma_2 D = \text{Cos}\gamma_2'' D$$

in equations (59) through (66) a corresponding set for the trigonometric case can be obtained.

Finally constants for electric and magnetic field expressions are determined as follows:

$$A^e(\alpha) = \frac{1}{k_{c_1}^2} E_z(\alpha) \tag{68}$$

$$A^h(\alpha) = \frac{1}{j\omega\mu_1\gamma_1} E_x(\alpha) + \frac{\alpha\gamma}{\omega\mu_1\gamma_1 k_{c_1}^2} E_z(\alpha) \tag{69}$$

$$C^e_{T,H}(\alpha) = 0 \tag{70}$$

$$B^h_{T,H}(\alpha) = 0 \tag{71}$$

$$B^e_T(\alpha) = \frac{1}{jk_{c_2}^2 \text{Sin}\gamma_2'' D} E_z(\alpha) \tag{72}$$

$$B^e_H(\alpha) = \frac{1}{k_{c_2}^2 \text{Sinh}\gamma_2 D} E_z(\alpha) \tag{73}$$

$$C^h_H(\alpha) = -\frac{1}{\omega\mu_2\gamma_2 \text{Sinh}\gamma_2 D}\left[\frac{\alpha\gamma}{k_{c_2}^2} E_z(\alpha) - jE_x(\alpha)\right] \tag{74}$$

$$C^h_T(\alpha) = \frac{1}{\omega\mu_2\gamma_2'' \text{Sin}\gamma_2'' D}\left[\frac{\alpha\gamma}{k_{c_2}^2} E_z(\alpha) - jE_x(\alpha)\right] \tag{75}$$

The subscript T denotes the trigonometric case and H denotes the Hyperbolic case. Substituting equations (70) through (75) into equation (65) and (66) one can obtain two sets of equations of the form

$$F_1(\alpha,\beta)E_x(\alpha) + F_2(\alpha,\beta)\ E_z(\alpha) = J_x(\alpha) \tag{76}$$

$$F_3(\alpha,\beta)E_x(\alpha) + F_4(\alpha,\beta)\ E_z(\alpha) = J_x(\alpha) \tag{77}$$

where

$$\gamma = j\beta.$$

For the hyperbolic case the F_i have the form

$$F_{1_H}(\alpha,\beta) = -j\left[\frac{k_{c_1}^2}{\omega\mu\gamma_1} + \frac{k_{c_2}^2}{\omega\mu_2\gamma_2}\ \text{Cotanh}\gamma_2 D\right] \tag{78}$$

$$F_{2_H}(\alpha,\beta) = j\left[\frac{\alpha\beta}{\omega\mu_1\gamma_1} + \frac{\alpha\beta}{\omega\mu_2\gamma_2}\ \text{Cotanh}\gamma_2 D\right] \tag{79}$$

$$F_{3_H}(\alpha,\beta) = -F_{2_H}(\alpha,\beta) \tag{80}$$

$$F_{4_H}(\alpha,\beta) = -j\left[-\frac{(\alpha\beta)^2}{\omega\mu_1\gamma_1 k_{c_1}^2} + \frac{\omega\varepsilon_1\gamma_1}{k_{c_1}^2} - \frac{\text{Cotanh}\gamma_2 D}{k_{c_2}^2}\left(\frac{(\alpha\beta)^2}{\omega\mu_2\gamma_2} - \omega\varepsilon_2\gamma_2\right)\right] \tag{81}$$

A similar set of equations for the trigonometric case can be obtained by use of equation (67). Solutions of equations (76) and (77) for $E_z(\alpha)$ and $E_x(\alpha)$ in terms of $J_z(\alpha)$ and $J_x(\alpha)$ may be obtained as follows:

$$E_x(\alpha) = \frac{F_4(\alpha,\beta)J_x(\alpha) - F_2(\alpha,\beta)J_z(\alpha)}{D_N} \tag{82}$$

$$E_z(\alpha) = \frac{-F_3(\alpha,\beta)J_x(\alpha) + F_1(\alpha,\beta)J_z(\alpha)}{D_N} \tag{83}$$

where

$$D_N = F_1(\alpha,\beta)F_4(\alpha,\beta) - F_2(\alpha,\beta)F_3(\alpha,\beta). \tag{84}$$

Define the following constants,

$$G_1(\alpha,\beta) = \frac{F_4(\alpha,\beta)}{D_N} \tag{85}$$

$$G_2(\alpha,\beta) = \frac{-F_2(\alpha,\beta)}{D_N} \tag{86}$$

$$G_3(\alpha,\beta) = \frac{-F_3(\alpha,\beta)}{D_N} \tag{87}$$

$$G_4(\alpha,\beta) = \frac{F_1(\alpha,\beta)}{D_N} \tag{88}$$

finally obtaining

$$E_x(\alpha) = G_1(\alpha,\beta)J_x(\alpha) \quad + G_2(\alpha,\beta)J_z(\alpha) \tag{89}$$

$$E_z(\alpha) = G_3(\alpha,\beta)J_x(\alpha) \quad + G_4(\alpha,\beta)J_z(\alpha). \tag{90}$$

C. PHYSICAL PARAMETERS

General equations (89) and (90) show no dependence on the actual physical configuration other than the boundary conditions.

In general, the transformed surface current densities $J_x(\alpha)$ and $J_z(\alpha)$ can be expanded in a set of known basis functions as,

$$J_x(\alpha) = \sum_{i=1}^{\infty} a_i j_{xi}(\alpha) \tag{91}$$

$$J_z(\alpha) = \sum_{i=1}^{\infty} b_i j_{zi}(\alpha). \tag{92}$$

Since the two conductors are sufficiently narrow, one may assume that the surface current density in the x-direction is zero. By modifying equations (89) and (90), also substituting (91) and (92) one obtains

$$G_2(\alpha,\beta) \sum_{i=1}^{\infty} b_i j_{zi}(\alpha) = E_x(\alpha) \tag{93}$$

$$G_4(\alpha,\beta) \sum_{i=1}^{\infty} b_i j_{zi}(\alpha) = E_z(\alpha). \tag{94}$$

Furthermore, although one could perform a multiterm approximation to the surface current density in the z-direction, in this case a one term approximation was found sufficient after different distributions were tried. For the numerical results of this present work uniform surface current density is used, thus

$$G_2(\alpha,\beta) b_1 j_{zi}(\alpha) = E_x(\alpha) \tag{95}$$

$$G_4(\alpha,\beta) b_1 j_{zi}(\alpha) = E_x(\alpha), \tag{96}$$

or substituting equation (92) for the case where i = 1,

$$G_2(\alpha,\beta) J_z(\alpha) = E_x(\alpha) \tag{97}$$

$$G_4(\alpha,\beta) J_z(\alpha) = E_z(\alpha). \tag{98}$$

It is clear that one only needs to work with either one of the above equations. Assuming a uniform current distribution

$$J_z(x) = \begin{cases} I_o/W & \text{on the strip} \\ 0 & \text{elsewhere} \end{cases}$$

where W is the width of the strip and I_o is the magnitude of the current, one can obtain the α-Domain Fourier transform, $\mathcal{J}_z(\alpha)$. This was done for three different configurations, namely single strip, coupled strips even mode and coupled strips odd mode.

For the geometry in Figure 3 one obtains the following:

<u>Single Strip</u>:

$$\mathcal{J}_z(\alpha) = \frac{I_o}{W} \int_{-W/2}^{W/2} e^{j\alpha x} dx, \quad \mathcal{J}_z(\alpha) = I_o \frac{\text{Sin}(\frac{\alpha W}{2})}{\frac{\alpha W}{2}} \tag{99}$$

<u>Coupled Strips, Even Mode</u>:

$$\mathcal{J}_z(\alpha) = \frac{I_o}{W} \int_{-(S/2+W)}^{-S/2} e^{j\alpha x} dx + \int_{S/2}^{(S/2+W)} e^{j\alpha x} dx$$

$$\mathcal{J}_z(\alpha) = 2I_o \text{Cos}\, \frac{\alpha(S+W)}{2} \quad \frac{\text{Sin}(\ \frac{\alpha W}{2}\ )}{(\ \frac{\alpha W}{2}\ )} \tag{100}$$

<u>Odd Mode</u>:

$$\mathcal{J}_z(\alpha) = \frac{I_o}{W} \int_{-(S/2+W)}^{-S/2} e^{j\alpha x} dx - \int_{S/2}^{-(S/2+W)} e^{j\alpha x} dx \tag{101}$$

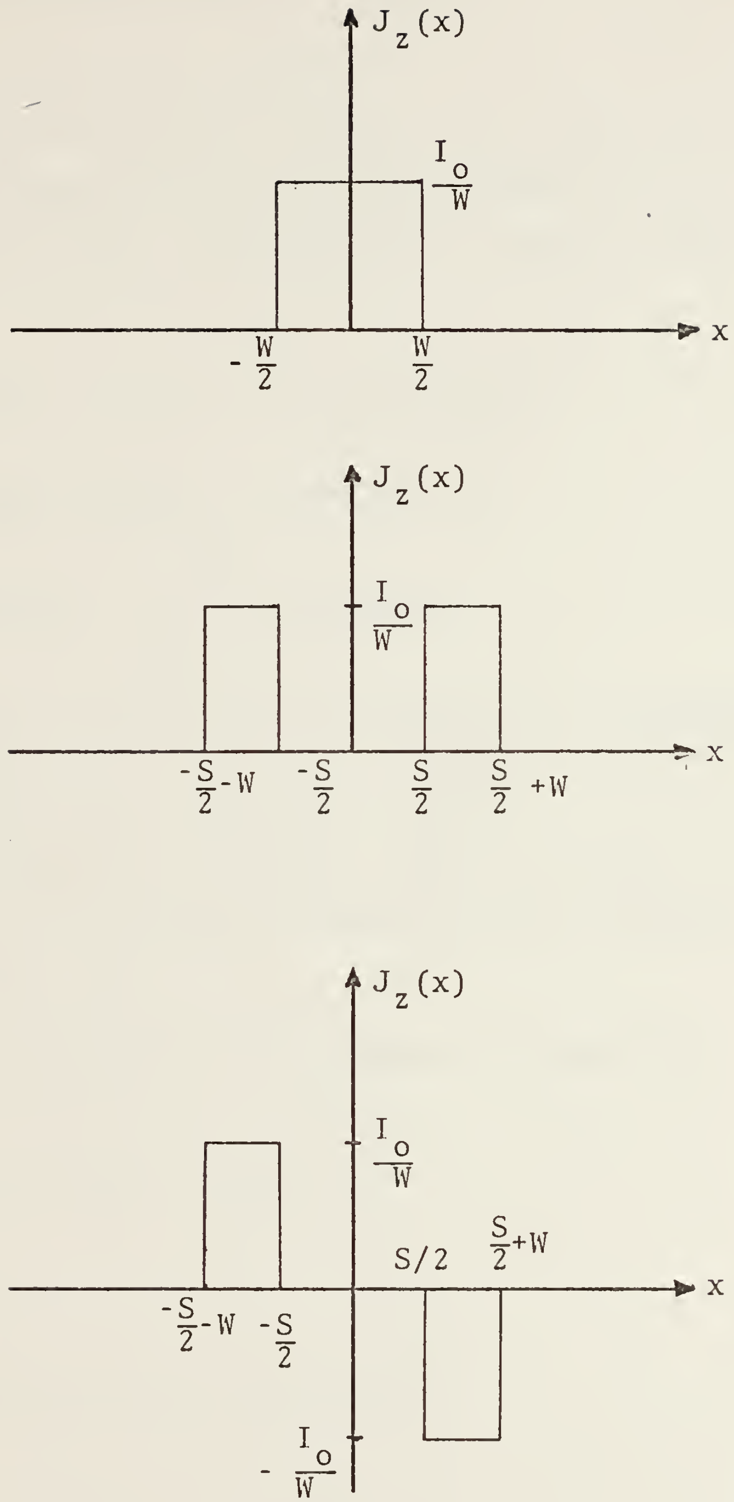

Figure 3. Single and Coupled Strips Even and Odd Longitudinal Current Distributions.

$$J_z(\alpha) = j2I_o \mathrm{Sin}\,\frac{\alpha(S+W)}{2} \quad \frac{\mathrm{Sin}(\alpha\frac{W}{2})}{(\frac{\alpha W}{2})} . \tag{101}$$

It is convenient to make equation (98) independent of $E_z(\alpha)$. This can be done by taking an inner product with a function orthogonal to $E_z(\alpha)$. Applying this concept, equation (98) becomes

$$\langle G_4(\alpha,\beta)J_z(\alpha),W(\alpha)\rangle = \langle E_z(\alpha),W(\alpha)\rangle \tag{102}$$

where the inner product is defined by

$$\langle Y(\alpha),W(\alpha)\rangle = \int_{-\infty}^{+\infty} Y(\alpha)W(\alpha)d\alpha. \tag{103}$$

A suitable weighting function $W(\alpha)$ is the complex conjugate of $J_z(\alpha)$; i.e. $J_z^*(\alpha)$ or $J_z(-\alpha)$.

Then by Parseval's theorem, the right-hand-side of equation (98) becomes zero because of the orthogonality of the $E_z(\alpha)$ and $J_z(\alpha)$.

Therefore equation (98) takes the final form

$$\int_{-\infty}^{+\infty} G_4(\alpha,\beta)J_z^*(\alpha)J_z(\alpha)d\alpha = 0 \tag{104}$$

or

$$\int_{-\infty}^{+\infty} G_4(\alpha,\lambda/\lambda')|J_z(\alpha)|^2 d\alpha = 0 \tag{105}$$

where

$$\beta = 2\pi/\lambda'.$$

So, one can see the integrand is dependent on the ratio of λ/λ' or effective dielectric constant, $\varepsilon_{r_{eff}}$, defined by

$$\varepsilon_{r_{eff}} = \left(\frac{\lambda}{\lambda'} \right)^2 .$$

Using the preceding current distributions for single and coupled lines, the phase velocity characteristics can be determined by finding those values of the propagation constant that give a zero value for the integral at a particular frequency.

It is clear that once equation (105) is integrated the dependence on the variable α disappears, so one can state that the whole process is really a function of frequency and the structure's physical characteristics, namely, width of the strips W, and in the case of coupled strips, separation S between the strips, thickness of substrate D, and the dielectric's relative permittivity ε_r.

By observing the behavior of each term equation (105) one can conclude integration of the $|J_z(\alpha)|^2$ term always gives a positive area. In the three configuration of microstrip which were studied, the Fourier transforms of the current distributions always provided a multiplicative factor of $(\mathrm{Sin}\alpha/\alpha)^2$ which gives rise to a curve having a large main lobe and low side lobes in the α-domain.

Several plots of $G_4(\alpha,\lambda/\lambda')$ and the $G_4(\alpha,\lambda/\lambda')\cdot|J_z(\alpha)|^2$ term between limits of α; $-3000<\alpha<3000$ for different λ/λ' values is shown in Figure 4 and Figure 5 respectively.

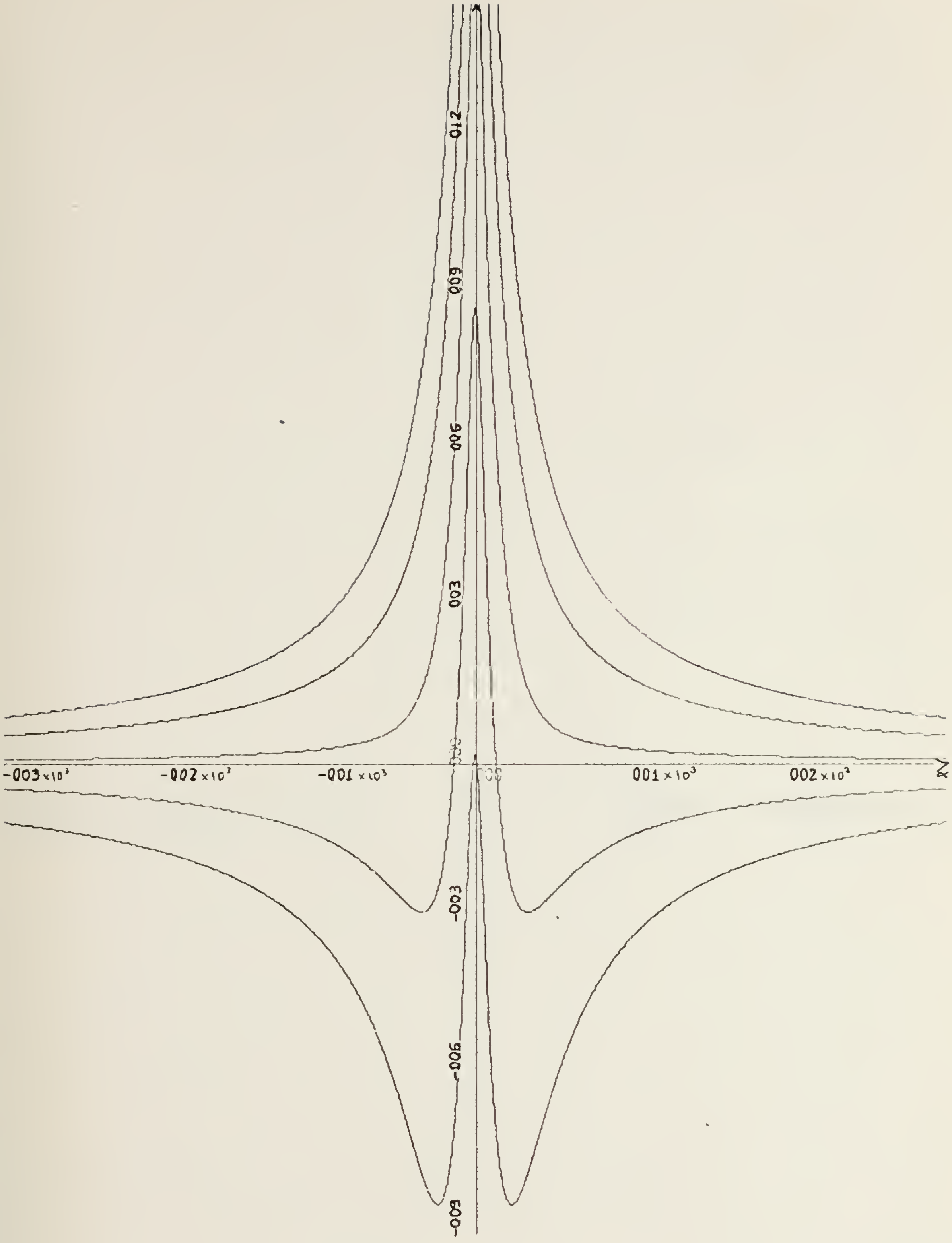

Figure 4. $G_4(\alpha,\lambda/\lambda')$ versus α.

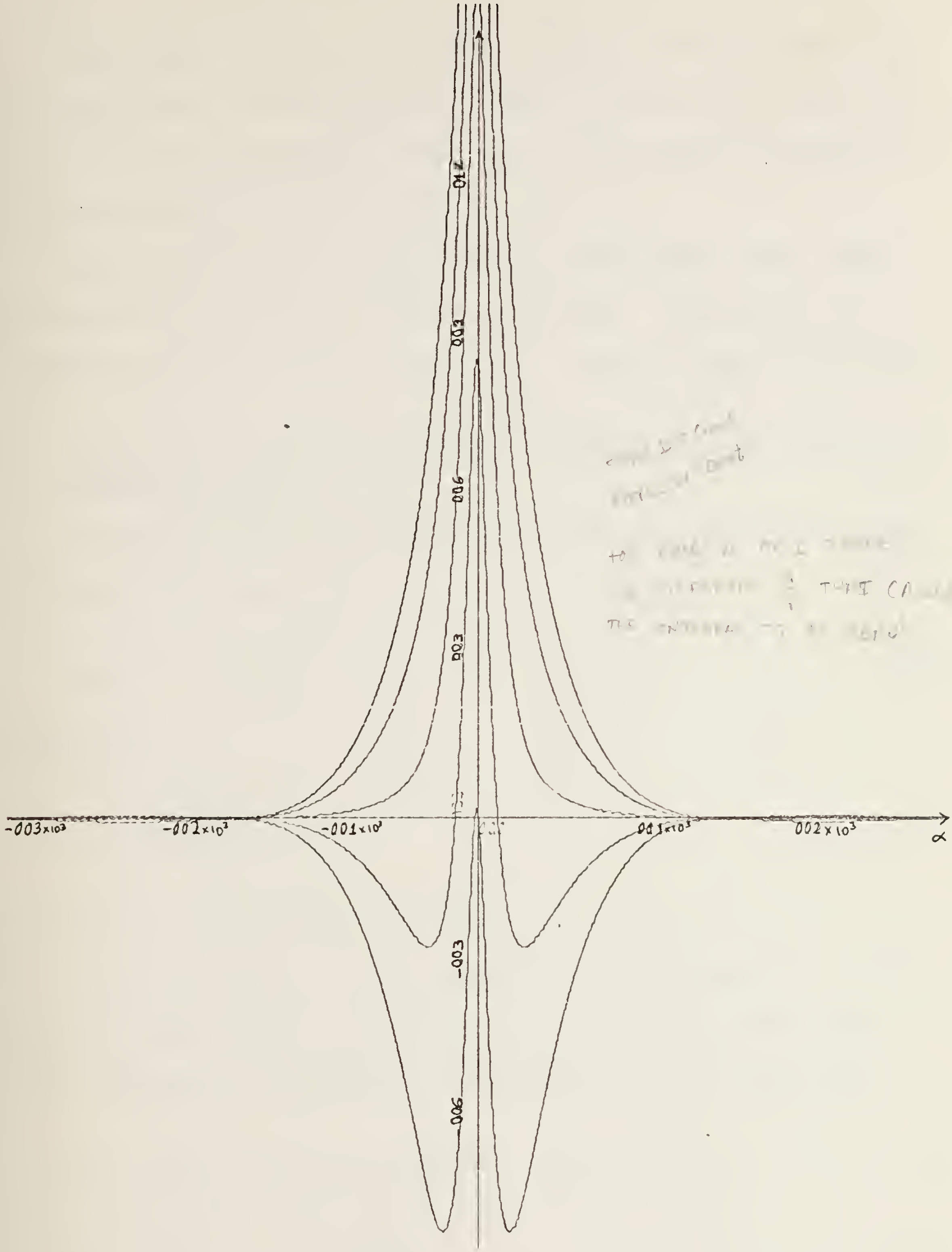

Figure 5. $G_4(\alpha,\lambda/\lambda')|J_z(\alpha)|^2$ versus α.

The family of curves is symmetrical to the y-axis and for decreasing values of λ/λ', moves along the y-axis without losing the symmetry. The total area under it monotonically decreases.

The value of λ/λ' which gives a zero total area under the curve is the root of equation (105). This gives the effective dielectric constant $\varepsilon_{r_{eff}}$ and the phase velocity.

D. THE CHARACTERISTIC IMPEDANCE IN TERMS OF THE DISPERSION CHARACTERISTICS

In general, one can express the average power in terms of the strip current as,

$$P_{AVE} = \frac{1}{2} I_{o_z}^2 Z_o \tag{106}$$

from which

$$Z_o = \frac{2P_{AVE}}{I_{o_z}^2} , \tag{107}$$

provided I_o is a unique current.

In this study, it was assumed in the dispersion characteristic part that the surface current across the strips were uniform; furthermore, the current can be expressed, as

$$I_{o_z} = \oint \overline{H}\cdot d\ell = \int_{STRIP} (H_{x_1} - H_{x_2}) dx \tag{108}$$

$$I_{o_z} = \int_{STRIP} |J_z(x)| dx. \tag{109}$$

In the case of a single strip,

$$J_z(x) = \begin{cases} \frac{I_o}{W} & \text{on the strips} \\ 0 & \text{elsewhere.} \end{cases}$$

For simplicity I_o is arbitrarily set equal to unity. Thus,

$$I_{o_z}^2 = 1. \tag{110}$$

As stated by Collin [Ref. 1], a general expression for the time average power flow in terms of the electric and magnetic fields is

$$P_{AVE}(x,y) = \mathrm{Re}\left[\tfrac{1}{2} \iint_S \bar{E} \times \bar{H}^{*} \cdot \bar{a}_z da \right] \tag{111}$$

where

$$\bar{E} \times \bar{H}^{*} \cdot \bar{a}_z = E_x H_y^{*} - E_y H_x^{*}.$$

This equation becomes

$$P_{AVE}(x,y) = \mathrm{Re}\left[\tfrac{1}{2} \iint_S (E_x H_y^{*} - E_y H_x^{*}) dxdy \right] \tag{112}$$

Referring back to equations (1) through (6), it is found that the equations for the electric and magnetic fields can be in terms of Hertzian potential functions.

So substituting equations (3) through (6) in the expression for average power,

$$P_{AVE}(x,y) = \tfrac{1}{2}\,\mathrm{Re}\left\{ \iint_S (j\beta\frac{\partial\phi^e}{\partial x} - j\omega\mu\frac{\partial\phi^h}{\partial y})e^{j\beta z}(-j\beta\frac{\partial\phi^h}{\partial y} \right. \tag{113}$$

$$+ j\omega\varepsilon\frac{\partial\phi^e}{\partial x})e^{-j\beta z}dxdy + \iint_S (j\beta\frac{\partial\phi^e}{\partial y} + j\omega\mu\frac{\partial\phi^h}{\partial x})e^{j\beta z}$$

$$\left.(-j\beta\frac{\partial\phi}{\partial x} - j\omega\varepsilon\frac{\partial\phi^e}{\partial y})e^{-j\beta z}dxdy\right\}. \tag{113}$$

Applying Parseval's theorem

$$P_{AVE} = \frac{1}{4\pi}\,\mathrm{Re}\left\{\int_{-\infty}^{+\infty}\int_{-\infty}^{+\infty}\left[\left(\alpha\beta\Phi^e(\alpha,y) - j\omega\mu\frac{\partial\Phi^h(\alpha,y)}{\partial y}\right)\right.\right.$$

$$\left(-j\beta\frac{\partial\Phi^{h*}(\alpha,y)}{\partial y} - \alpha\omega\varepsilon\Phi^{e*}(\alpha,y)\right) - \left(j\beta\frac{\partial\Phi^e(\alpha,y)}{\partial y} + \alpha\omega\mu\Phi^h(\alpha,y)\right)$$

$$\left.\left.\left(\beta\alpha\Phi^{h*}(\alpha,y) - j\omega\varepsilon\frac{\partial\Phi^{*e}(\alpha,y)}{\partial y}\right)\right]d\alpha dy\right\}. \tag{114}$$

where the Fourier transform of $\partial\phi/\partial x$ has been applied from equation (114). Performing the operations indicated,

$$P_{AVE} = \frac{1}{4\pi}\,\mathrm{Re}\left\{\int_{-\infty}^{+\infty}\int_{-\infty}^{+\infty}\left[-\alpha^2\beta\omega\varepsilon|\Phi^e(\alpha,y)|^2 - \omega\beta\mu\left|\frac{\partial\Phi^h(\alpha,y)}{\partial y}\right|^2\right.\right.$$

$$- \omega\beta\varepsilon\left|\frac{\partial\Phi^e(\alpha,y)}{\partial y}\right|^2 - \alpha^2\omega\mu\beta|\Phi^h(\alpha,y)|^2$$

$$+ j\alpha k^2\left(\Phi^h(\alpha,y)\frac{\partial\Phi^{*e}(\alpha,y)}{\partial y} + \Phi^{e*}(\alpha,y)\frac{\partial\Phi^h(\alpha,y)}{\partial y}\right) \tag{115}$$

$$\left.\left.- j\alpha\beta^2\left(\Phi^e(\alpha,y)\frac{\partial\Phi^{h*}(\alpha,y)}{\partial y} + \Phi^{h*}(\alpha,y)\frac{\partial\Phi^e(\alpha,y)}{\partial y}\right)\right]d\alpha dy\right\}$$

where

$$k^2 = \omega^2\mu\varepsilon.$$

After obtaining the general expression for average power, one can apply it to both regions for further specific equations.

In Region 1,

$$\Phi_1^e(\alpha,y) = A^e(\alpha)e^{-\gamma_1(y-D)} \tag{116}$$

$$\Phi_1^h(\alpha,y) = A^h(\alpha)e^{-\gamma_1(y-D)} \tag{117}$$

$$\frac{\partial\Phi_1^e(\alpha,y)}{\partial y} = -\gamma_1 A^e(\alpha)e^{-\gamma_1(y-D)} \tag{118}$$

$$\frac{\partial\Phi_1^h(\alpha,y)}{\partial y} = -\gamma_1 A^h(\alpha)e^{-\gamma_1(y-D)} \tag{119}$$

Substituting the preceding equations in (115) one can obtain

$$P_{1_{AVE}} = \frac{1}{4\pi}\,\mathrm{Re}\Bigg\{\int_{-\infty}^{+\infty}\int_{D}^{+\infty} e^{-2\gamma_1(y-D)}\Big[-\alpha^2\mu\omega\varepsilon_1|A^e(\alpha)|^2 \tag{120}$$

$$-\omega\beta\mu_1\gamma_1^2|A^h(\alpha)|^2 - \omega\beta\varepsilon_1\gamma_1^2|A^e(\alpha)|^2 - \alpha^2\omega\mu_1\beta|A^h(\alpha)|^2$$

$$-j\alpha k_1^2(2\gamma_1 A^h(\alpha)A^{e*}(\alpha)) + j\alpha\beta^2(2\gamma_1 A^e(\alpha)A^{h*}(\alpha))\Big]\,d\alpha dy\Bigg\}.$$

It is clear from the above expression that one can integrate with respect to y to obtain

$$P_{1_{AVE}} = -\frac{1}{8\pi}\int_{-\infty}^{+\infty}\Bigg[\left(\frac{\alpha^2+\gamma_1^2}{\gamma_1^2}\right)\Bigg(\beta\omega\varepsilon_1|A^e(\alpha)|^2 \tag{121}$$

$$+\beta\omega\mu_1|A^h(\alpha)|^2 + 2\alpha(\beta^2+k_1^2)\,\mathrm{Re}\left\{-jA^e(\alpha)A^{*h}(\alpha)\right\}\Bigg)\Bigg]\,d\alpha.$$

In Region 2, clearly there are two expressions for average power. When γ_2 is real, equations (47) and (49) apply as stated earlier.

$C_{T,H}(\alpha)$ and $B^h_{T,H}(\alpha)$ are zero so,

$$\Phi^e_2(\alpha,y) = B^e_H(\alpha)\,\mathrm{Sinh}\gamma_2 y \tag{122}$$

$$\Phi^h_2(\alpha,y) = C^h_H(\alpha)\,\mathrm{Cosh}\gamma_2 y \tag{123}$$

$$\frac{\partial\Phi^h_2(\alpha,y)}{\partial y} = \gamma_2 C^h_H(\alpha)\,\mathrm{Sinh}\gamma_2 y \tag{124}$$

$$\frac{\partial\Phi^e_2(\alpha,y)}{\partial y} = \gamma_2 B^e_H(\alpha)\,\mathrm{Cosh}\gamma_2 y \tag{125}$$

and

$$\begin{aligned} P_{2_{AVE_H}} = -\frac{1}{4\pi}\,\mathrm{Re}\Bigg\{ \iint_{\substack{\text{HYP}\\ \text{REGION}}}\int_0^D & \mathrm{Sinh}^2\gamma_2 y\,[\alpha^2\beta\omega\varepsilon_2|B^e_H(\alpha)|^2 \\ & + \beta\omega\mu_2\gamma_2^2|C^h_H(\alpha)|^2 + j\alpha\beta^2\gamma_2 B^e(\alpha)C^{h*}_H(\alpha) \\ & - j\alpha\gamma_2 k_2^2 C^h_H(\alpha)B^{e*}_H(\alpha)]\,d\alpha dy + \mathrm{Cosh}^2\gamma_2 y \\ & [\alpha^2\beta\omega\mu_2|C^h_H(\alpha)|^2 + \beta\omega\varepsilon_2\gamma_2^2|B^e_H(\alpha)|^2 \\ & + j\alpha\beta^2\gamma_2 B^e_H(\alpha)C^{h*}_H(\alpha) - j\alpha k_2^2\gamma_2 C^h_H(\alpha)B^{e*}_H(\alpha)]\,d\alpha dy\Bigg\}\,. \end{aligned} \tag{126}$$

The y-dependence of the average power in Region 2 disappears through corresponding integrations as indicated below:

$$\int_0^D \mathrm{Sinh}^2\gamma_2 y\,dy = \frac{\mathrm{Sinh}2\gamma_2 D - 2\gamma_2 D}{2\gamma_2} \tag{127}$$

$$\int_0^D \mathrm{Cosh}^2\gamma_2 y\,dy = \frac{\mathrm{Sinh}2\gamma_2 D + 2\gamma_2 D}{2\gamma_2} \quad . \tag{128}$$

Thus,

$$P_{2_{AVE_H}} = -\frac{1}{16\pi}\,\mathrm{Re}\left\{\int_{\substack{HYP\\REGION}} (\mathrm{Sinh}2\gamma_2 D - 2\gamma_2 D)\right.$$

$$\left[\frac{\alpha^2\beta\omega\varepsilon_2}{\gamma_2}\,|B_H^e(\alpha)|^2 + \beta\omega\mu_2\gamma_2|C_H^h(\alpha)|^2\right.$$

$$\left. + j\alpha\beta^2 B_H^e(\alpha)C_H^{*h}(\alpha) - j\alpha k_2^2 C_H^h(\alpha)B_H^{*e}(\alpha)\right]d\alpha$$

$$+ \int_{\substack{HYP\\REGION}} (\mathrm{Sinh}2\gamma_2 D + 2\gamma_2 D)\left[\frac{\alpha^2\beta\omega\mu_2}{\gamma_2}\,|C_H^h(\alpha)|^2\right.$$

$$+ \beta\omega\varepsilon_2\gamma_2|B_H^e(\alpha)|^2 + j\alpha\beta^2 B_H^e(\alpha)C_H^{*h}(\alpha)$$

$$\left.\left. - j\alpha k_2^2 C_H^h(\alpha)B_H^{e*}(\alpha)\right]d\alpha\right\} \quad . \tag{129}$$

It is also clear that for imaginary γ_2 the average power expression can easily be obtained with substitution of (48) and (50) and the corresponding trigonometric case electric and magnetic field constants i.e. equation (72) and (74). A detailed exposure to such analysis is given in Appendix C.

Then for imaginary γ_2 Region 2:

$$P_{2_{AVE_T}} = -\frac{1}{16\pi} \mathrm{Re}\Bigg\{ \int_{\substack{\mathrm{TRIG}\\ \mathrm{REGION}}} (2\gamma_2''D - \mathrm{Sin}2\gamma_2''D)\Big[\frac{\alpha^2\beta\omega\varepsilon_2}{\gamma_2''}$$

$$|B_T^e(\alpha)|^2 + \beta\omega\mu_2\gamma_2''|C_T^h(\alpha)|^2 + \alpha\beta^2 B_T^e(\alpha)C_T^{*h}(\alpha)$$

$$+ \alpha k_2^2 C_T^h(\alpha)B_T^{*e}(\alpha)\Big]d\alpha + \int_{\substack{\mathrm{TRIG}\\ \mathrm{REGION}}} (2\gamma_2''D + \mathrm{Sin}2\gamma_2''D)$$

$$\Big[\frac{\alpha^2\beta\omega\mu_2}{\gamma_2''}|C_T^h(\alpha)|^2 + \beta\omega\varepsilon_2\gamma_2''|B_T^e(\alpha)|^2 - \alpha\beta^2 B_T^e(\alpha)C_T^{*h}(\alpha)$$

$$- \alpha k_2^2 C_T^h(\alpha)B_T^{e*}(\alpha)\Big]d\alpha\Bigg\}. \tag{130}$$

Total power in Region 2 becomes:

$$P_{2_{AVE}} = P_{2_{AVE_H}} + P_{2_{AVE_T}}. \tag{131}$$

As strip width decreases one observes a widening α-domain power distribution in Region 1. Also for higher values of dielectric constant where the energy is more concentrated into the substrate, a wider α-domain power distribution is obtained in Region 2.

Finally, characteristic impedance can be found as

$$Z_0 = \frac{2(P_{1_{AVE}} + P_{2_{AVE}})}{I_{o_z}^2} \tag{132}$$

In all cases, geometry is taken into account in the current distribution expressions.

Plots of α-domain power distribution for Regions 1 and 2 are shown in Figure 6 and Figure 7 respectively. By

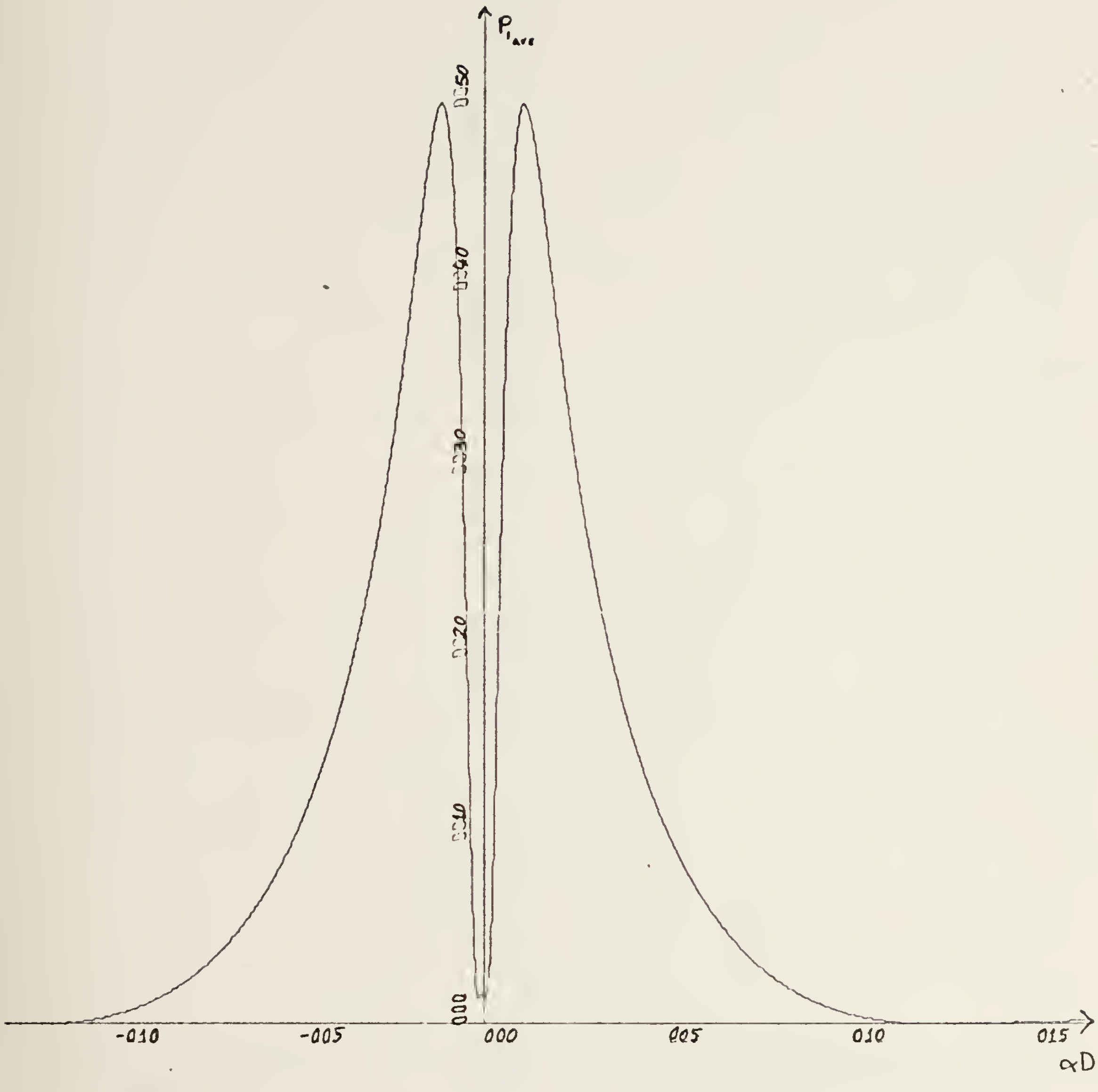

Figure 6. Region 1 Average Power Distribution in α-Domain.

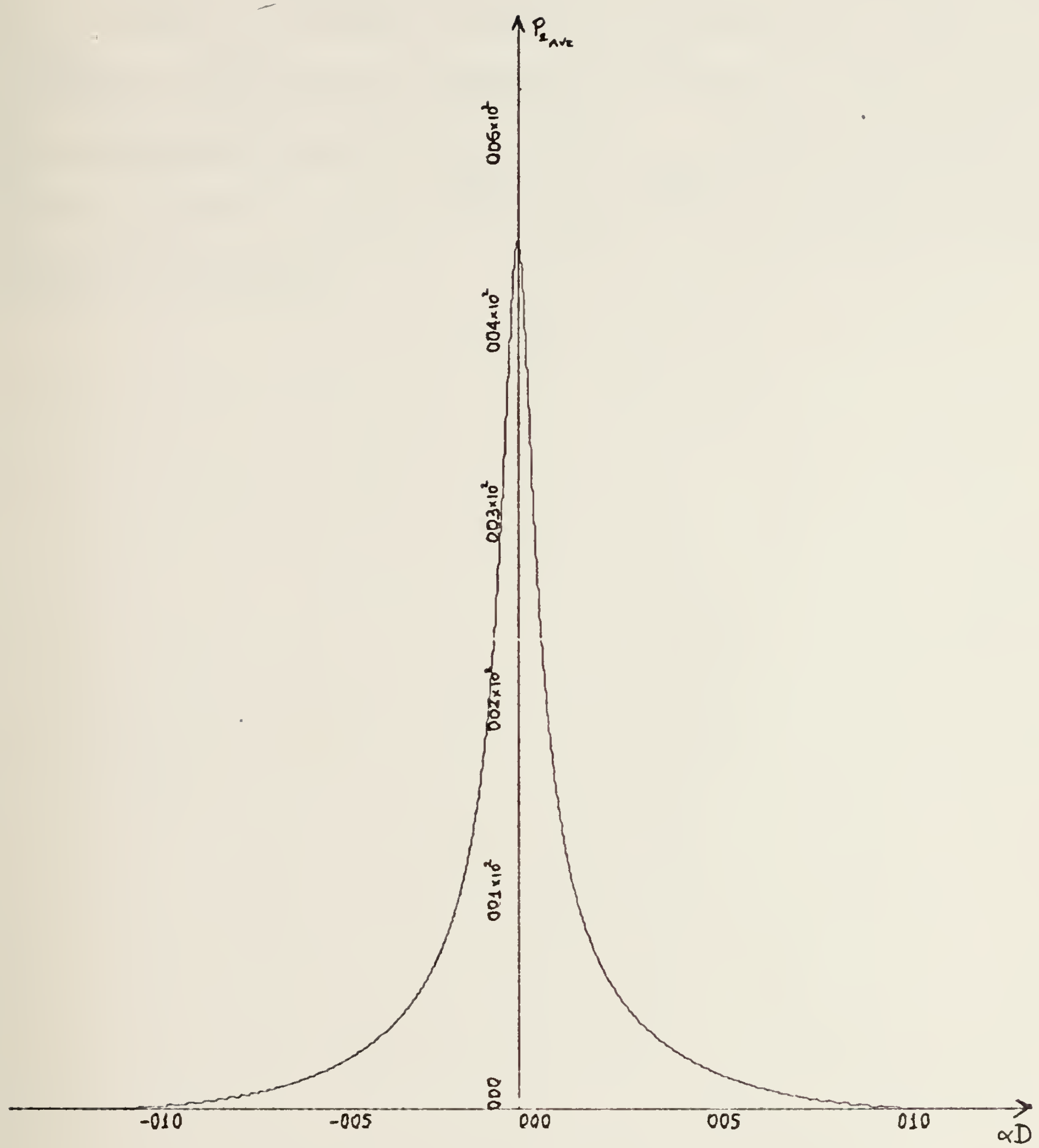

Figure 7. Region 2 Average Power Distribution in α-Domain.

taking the inverse Fourier transforms of $P_{1_{AVE}}$ and $P_{2_{AVE}}$ one could obtain the x-domain power distribution.

It is important to observe and prove the continuation of $P_{1_{AVE}}$ and $P_{2_{AVE}}$ curves for the critical points where γ_2 switches from real to imaginary character or vice versa. The enlarged views of $P_{1_{AVE}}$ and $P_{2_{AVE}}$ given in Figures 8 and 9 clearly show the smoothness of transition from one region to another.

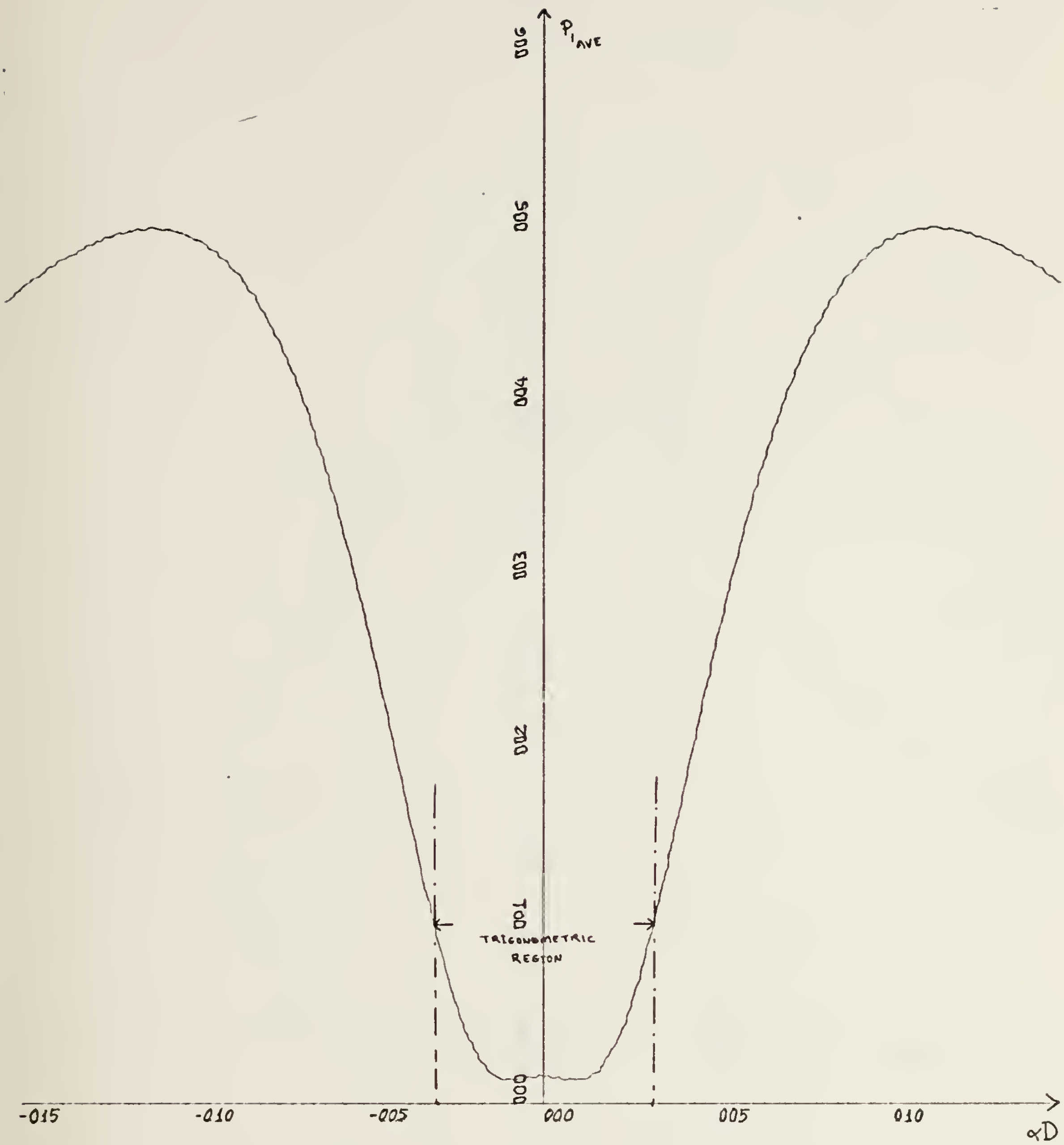

X-SCALE=5.00E-01 UNITS INCH.
Y-SCALE=1.00E+01 UNITS INCH.

Figure 8. $P_{1_{AVE}}$ versus αD at 1 GHz.

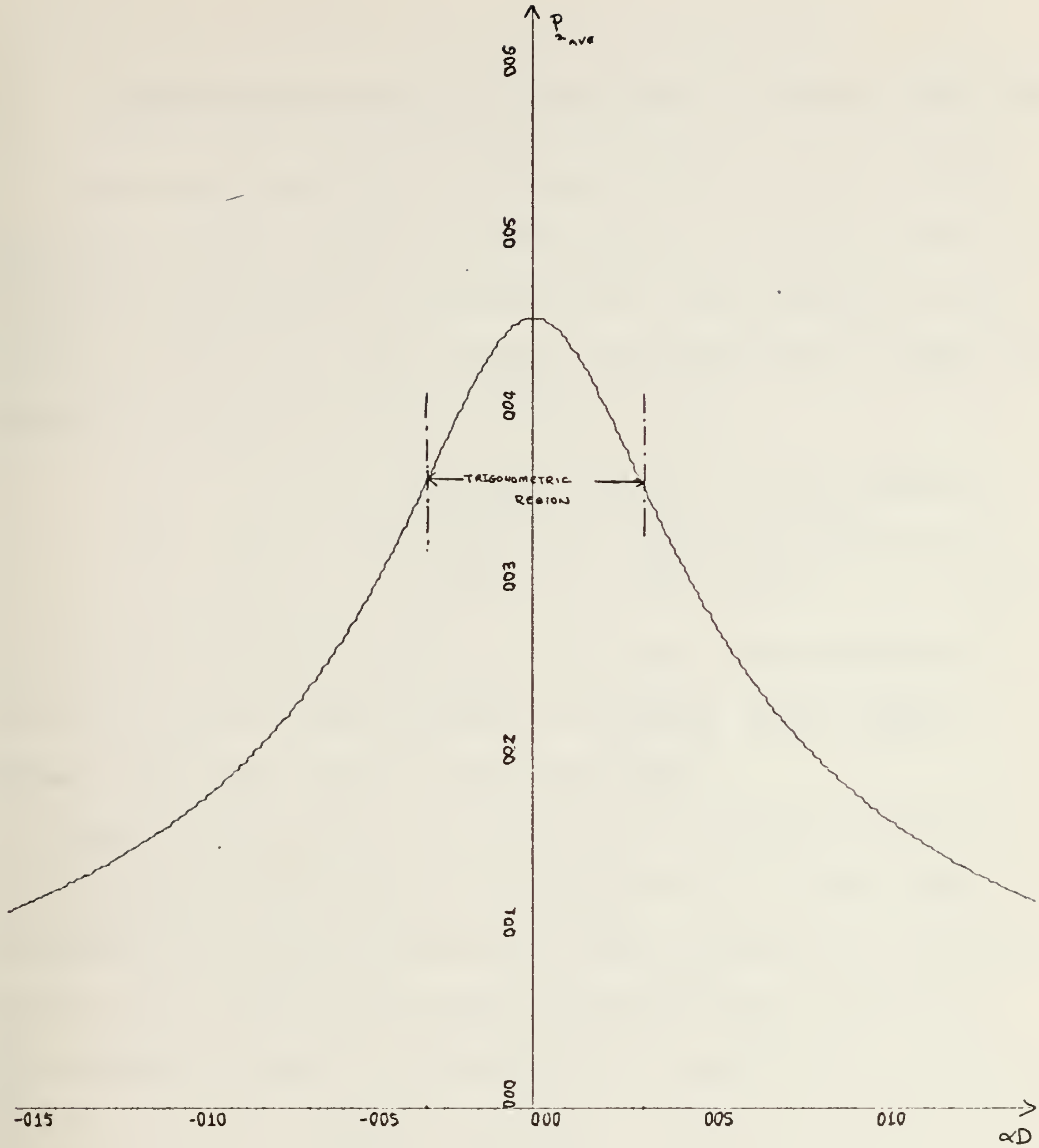

X-SCALE=5.00E-01 UNITS INCH
Y-SCALE=1.00E+02 UNITS INCH

Figure 9. $P_{2_{AVE}}$ versus αD at 1 GHz.

III. PERTURBATION ANALYSIS OF MICROSTRIP ON FERRITE SUBSTRATE

Considered here is an extension of the spectral domain technique to the analysis of microstrip on a ferrite substrate. A familiar perturbation expression for the propagation constant of a hollow, closed boundary waveguide with a change in material is given by Helszajn [Ref. 5] as:

$$(\Gamma' + \Gamma^*) = \frac{j\omega \iint_s (\varepsilon_o [\Delta\chi_e]\cdot\overline{E}'\cdot\overline{E}^* + \mu_o \, [\Delta\chi_m]\cdot\overline{H}'\cdot\overline{H}^*)da}{\iint_s (\overline{E}^* \times \overline{H}' + \overline{E}'\times\overline{H}^*)\cdot\overline{a}_z \, da} \tag{133}$$

which primes denote perturbed quantities. This expression also is valid for open boundary structures which support bound waves [Ref. 7] as is the case here.

Consider the case of a microstrip on ferrite with magnetization perpendicular to the substrate. In this case, assuming the lossless dielectric substrate problem is solved, there is no change in electric susceptibility so $[\Delta\chi_e] = 0$. The change in magnetic susceptibility is given by

$$[\Delta\chi_m] = \begin{bmatrix} \chi_{xx} & 0 & \chi_{xz} \\ 0 & 0 & 0 \\ \chi_{zx} & 0 & \chi_{zz} \end{bmatrix} \tag{134}$$

where magnetic loss is permitted. The denominator of (133) is just $4P_{AVG}$ so one obtains

$$\Gamma' + \Gamma^* = j\omega\mu_o \frac{\iint_s [\Delta\chi_m]\cdot\overline{H}'\cdot\overline{H}^* da}{2Z_o I_{o_z}^2} . \tag{135}$$

Evaluation of the numerator of (135) leads to:

$$\Gamma' + \Gamma^* = j\omega\mu_o \frac{\int_{-\infty}^{+\infty}\int_0^D (\chi_{xx}H_xH_x^* + \chi_{zz}H_zH_z^*)\,dy\,dx}{2Z_oI_{o_z}^2} \tag{136}$$

where unperturbed fields have been used as a first approximation to perturbed fields and where because of the geometry no demagnetization of r.f. fields takes place. No cross terms involving products of H_z and H_x appear in the numerator of (136) because this product is odd and

$$\int_{-\infty}^{+\infty} H_zH_x^*dx = \int_{-\infty}^{+\infty} H_xH_z^*dx = 0. \tag{137}$$

Referring back to equations (2) and (5), substituting in equation (136) and applying the Parseval's theorem one obtains:

$$\Gamma' + \Gamma^* = \frac{j\omega\mu_o}{2Z_oI_{o_z}^2}\ \frac{1}{2\pi}\int_{-\infty}^{+\infty}\int_0^D \Bigg\{ \chi_{xx}\Bigg[\pm j\beta(-j\alpha\Phi_2^h(\alpha,y) + j\omega\varepsilon_2\frac{\partial\Phi_2^e(\alpha,y)}{\partial y}\Bigg]\Bigg[\mp j\beta(-j\alpha\Phi_2^h(\alpha,y) - j\omega\varepsilon_2\frac{\partial\Phi_2^e(\alpha,y)}{\partial y})\Bigg]^* + \chi_{zz}k_{c_2}^4\Phi_2^h(\alpha,y)\Phi_2^{h*}(\alpha,y)\Bigg\}\,dy\,d\alpha \tag{138}$$

where

$$\chi_{zz} = \chi_{xx}.$$

This propagation constant expression holds for $\pm$ z directed traveling waves depending upon the choice of upper or lower sign in (138).

One might attempt to solve this equation by defining regions of α where γ_2 has imaginary and real values which are indicated by equations (36) and (37).

Also substituting previously calculated corresponding equations of $\Phi_2^h(\alpha,y)$ and $(\partial\Phi_2^e(\alpha,y))/\partial y$ for hyperbolic and trigonometric cases into (138) and integrating out the y dependence the following is obtained:

$$\Gamma' + \Gamma^* = \frac{1}{16\pi} \cdot \frac{j\omega\mu_o}{Z_o I_{o_z}^2} \int_{\substack{\text{TRIG}\\\text{REGION}}} \left(\frac{2\gamma_2'' D + \sin 2\gamma_2'' D}{\gamma_2''}\right)$$

$$\Big\{ \chi_{xx} [(-\beta^2\alpha^2 + k_{c_2}^4) | C_T^h(\alpha)|^2 \pm j\omega\varepsilon_2\beta\alpha\gamma_2''$$

$$(-jC_T^h(\alpha)B_T^{*e}(\alpha) - jC_T^{h*}(\alpha)B_T^e(\alpha)) - (\omega\varepsilon_2\gamma_2'')^2 |B_T^e(\alpha)|^2$$

$$\Big\} d\alpha + \frac{1}{16\pi} \frac{j\omega\mu_o}{Z_o I_{o_z}^2} \int_{\substack{\text{HYP}\\\text{REGION}}} \left(\frac{\sinh 2\gamma_2 D - 2\gamma_2 D}{\gamma_2}\right)$$

$$\Big\{ \chi_{xx} [(-\beta^2\alpha^2 + k_{c_2}^4) |C_H^h(\alpha)|^2 \pm j\omega\varepsilon_2\beta\alpha\gamma_2 (C_H^h(\alpha)B_H^{e*}(\alpha)$$

$$- C_H^{h*}(\alpha)B_H^e(\alpha)) - (\omega\varepsilon_2\gamma_2)^2 |B_H^e(\alpha)|^2] \Big\} d\alpha. \qquad (139)$$

Evaluating the difference between perturbed and inperturbed propagation constants,

$$\begin{aligned} \Gamma' + \Gamma^* &= \Delta\alpha + j\Delta\beta \\ \Gamma' + \Gamma^* &= \alpha' + j\beta' - j\beta \end{aligned} \qquad (140)$$

where

$\Delta\alpha = \alpha'$ and $\Delta\beta = \beta' - \beta$.

Also, as stated in Reference 5

$$\chi_{xx} = \chi'_{xx} - j\chi''_{xx}. \tag{141}$$

Substituting (140) and (141) into equation (139) and separating real and imaginary parts gives expressions for α' and β', loss and phase shift with ferrite respectively.

Define a common expression

$$K^{\mp} = \frac{1}{16\pi} \cdot \frac{j\omega\mu_o}{Z_o I_{o_z}^2} \left\{ \int_{\substack{\text{TRIG}\\\text{REGION}}} \left(\frac{2\gamma_2'' + \mathrm{Sin}\, 2\gamma_2'' D}{\gamma_2''}\right) \left[(-\beta^2\alpha^2 + k_{c_2}^4) \left|C_T^h(\alpha)\right|^2 \pm 2\omega\varepsilon_2 \beta\alpha\gamma_2'' (C_T^h(\alpha) B_T^{e*}(\alpha)) - (\omega\varepsilon_2\gamma_2'')^2 \left|B_T^e(\alpha)\right|^2 \right] d\alpha + \int_{\substack{\text{HYP}\\\text{REGION}}} \left(\frac{\mathrm{Sinh}\, 2\gamma_2 D - 2\gamma_2 D}{\gamma_2}\right) \left[(-\beta^2\alpha^2 + k_{c_2}^4) \left|C_H^h(\alpha)\right|^2 \pm 2\omega\varepsilon_2\beta\alpha\gamma_2 (-jC_H^{*h}(\alpha) B_H^e(\alpha)) - (\omega\varepsilon_2\gamma_2)^2 \left|B_H^e(\alpha)\right|^2 \right] d\alpha \right\} \tag{142}$$

Then

$$\Delta\alpha^{\mp} = K^{\mp}\chi''_{xx} \tag{143}$$

$$\Delta\beta^{\mp} = K^{\mp}\chi'_{xx} \tag{144}$$

where χ'_{xx} and χ''_{xx} are defined in Reference 5.

Loss in db per wavelength versus frequency and β_f/β versus frequency are plotted in Figures 10 and 11.

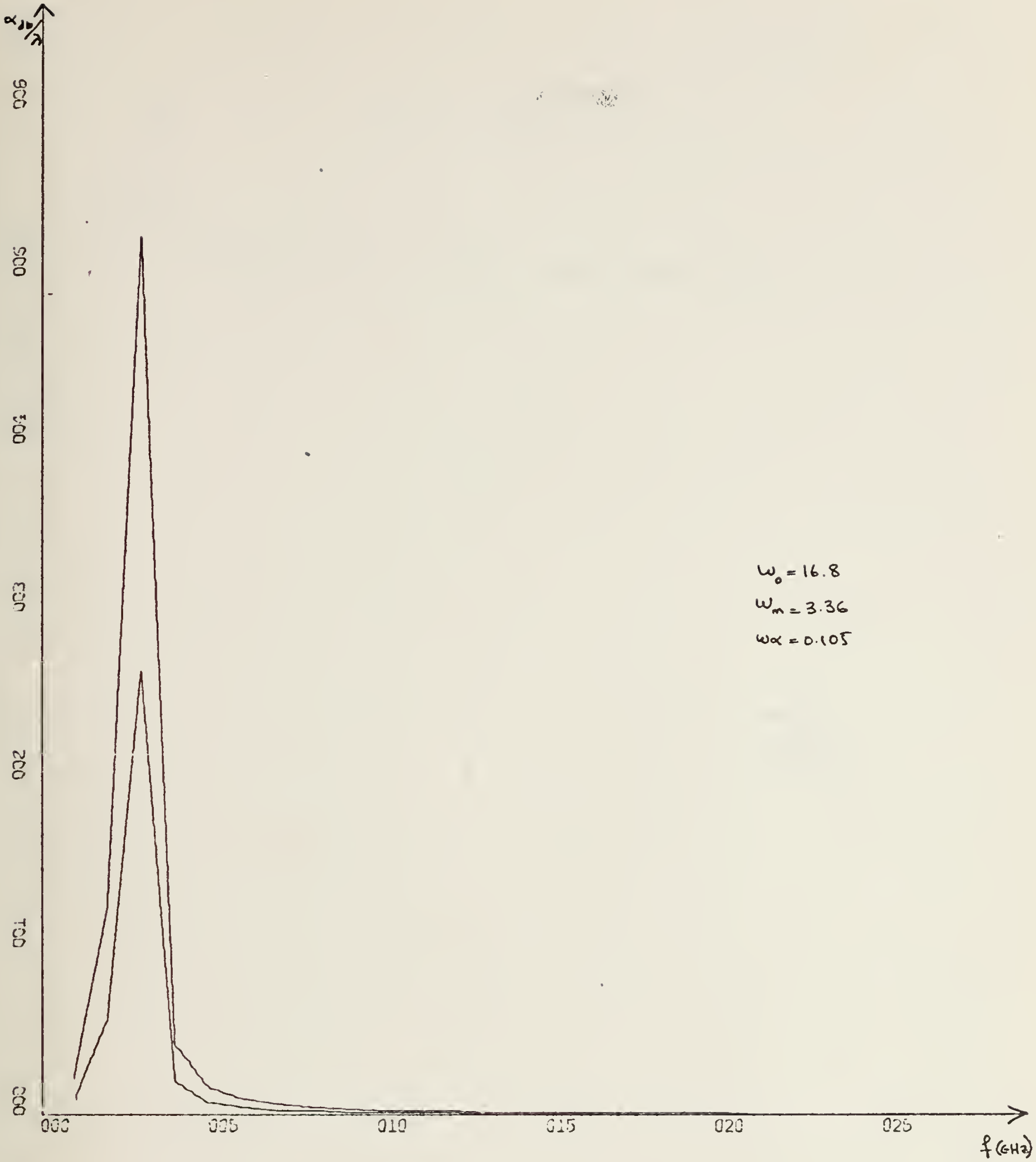

X-SCALE=5.00E+00 UNITS INCH.
Y-SCALE=1.00E-01 UNITS INCH.

Figure 10. Loss per wavelength in db versus frequency (GHz).

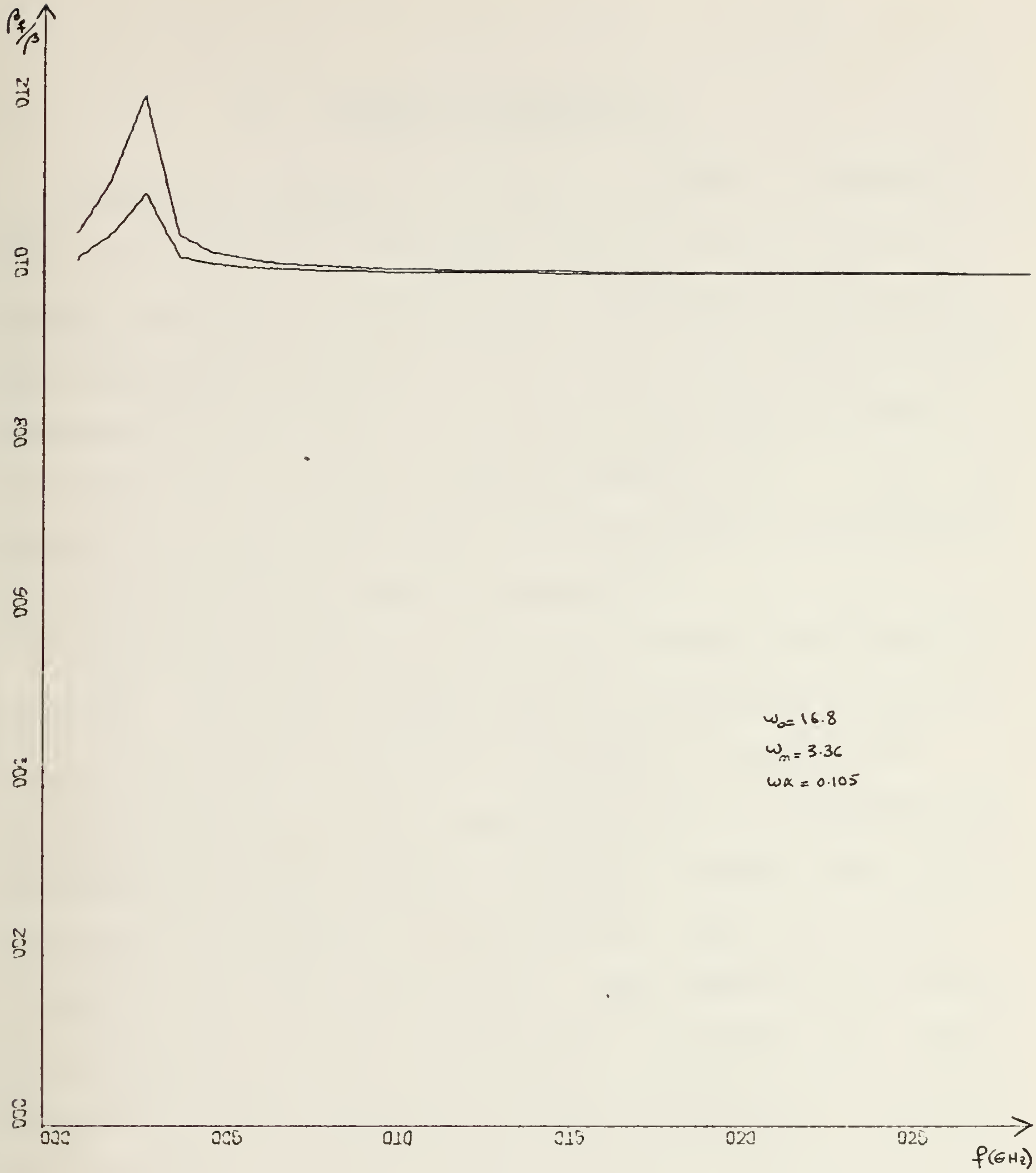

X-SCALE=5.00E+00 UNITS INCH.
Y-SCALE=2.00E-01 UNITS INCH.

Figure 11. β_f/β versus frequency (GHz).

IV. COMPUTER PROGRAMMING

A computer program is written in FORTRAN IV language that first calculates the phase velocity or λ/λ' ratio for a given geometry of microstrip and parameters of substrate. Then the program proceeds and calculates the characteristic impedance for the same set of data using results found in the first phase of the calculation namely λ/λ'. If the substrate is ferrite, also phase shift and loss per wavelength are calculated and curves are generated.

The program consists of one main routine and three subroutines. The main routine starts by calculating all constants and parameters which are needed to evaluate the various integrals. First equation (105) is integrated and evaluated for an arbitrary initial λ/λ' value. This process continues for different values of λ/λ' until zero is obtained as the value of integral. This computer time consuming iteration process is shortened by a simple root finding routine that determines the correct region of λ/λ' and eliminates others. On the average, after 9 iterations equation (105) gives a value which will yield zero value for the integral with an accuracy of 0.01%. The exact number of steps will change depending on desired accuracy and physical parameters.

Evaluation of the integral is done by standard IBM 360/67 system library subroutine DQG24 which uses a 24

point Gaussian Quadrature formula which integrates polynomials up to 47th degree.

This routine has been found to accurately integrate the type of curves encountered in this study.

The DQG24 routine requires an external function subprogram which defines the polynomial to be integrated for imaginary and real values of γ_2. Two different subprograms GZR, GZIM were used for this purpose and to test and set the limits of integration, for real and imaginary character of γ_2 respectively.

It is also proven that increasing the limits of integration or using a 32 point integration routine which evaluates polynomials up to 64th degree does not change the result more than 0.1%.

Another subroutine called TRAN supplies the expression for the transformed current distribution depending upon the physical configuration of the microstrip.

As far as the theoretical development and programming is concerned the only approximations used are the representation of the axial surface current density by a square pulse and the assumption that the transverse surface current density is zero. Different forms of current distributions were tried such as

$$J_z(x) = \begin{cases} \cosh x & \text{on the strip} \\ 0 & \text{elsewhere.} \end{cases}$$

It was concluded that due to the many zero crossings of this transformed current distribution curve and the greater number of side lobes which adversely affected programming efficiency its use was not justified even though it more accurately approximates the true current distribution.

Characteristic impedance was calculated as a next step by evaluating equations (129), (130) and (132) using different parts of the same routines used in the first part of the calculation.

If the substrate is ferrite the program proceeds to another section which evaluates equations (142) through (144) and calculates loss and phase shift values as a function of operation frequency.

It may be pertinent to quote the typical computational time using the method outlined in this study.

From the GO step the average time for calculating λ/λ', Z_o, and loss and phase shift (if necessary) for a single frequency was between 1.5 to 1.9 sec on an IBM 360/67.

The computer program accepts the following data:

- Substrate parameters, ε_{r_2}, μ_{r_2}.
- Thickness of substrate, D, in millimeters.
- The separation between conductors, S, in millimeters (only for coupled strip).
- Initial frequency (GHz).

The program starts calculating values for the initial frequency and repeats the procedure by increasing the frequency in 1 GHz steps up to 50 times. Means are also provided to compare the half wavelength, $\lambda/2$, with the thickness

of the substrate, D. For

$$D = \frac{\lambda}{2}$$

the program stops due to the presence of higher order modes.

V. NUMERICAL RESULTS AND COMPARISONS

The dispersion characteristic of the microstrip as a function of frequency has been evaluated for a variety of geometries and these results are presented both in tabular and plotted form. In addition, characteristic impedance as a function of frequency is presented for the same geometries and dielectric constant.

Figures 12 through 15 show the frequency variation of wavelength and characteristic impedance of a single strip for various values of W/D. Similar families of curves for coupled strips appear in Figures 16 through 19. In this case the parameter is S/D and W/D is held constant.

The results indicate that higher frequencies and wider strips increase the effective dielectric constant, $\varepsilon_{r_{eff}}$, and the characteristic impedance Z_o of both single and coupled strips. The spacing S between coupled strips also has an effect on $\varepsilon_{r_{eff}}$. Increasing spacing, S, increases $\varepsilon_{r_{eff}}$ for odd and even modes. The effect on characteristic impedance depends upon the mode of propagation. Increasing spacing, S, increases Z_o for the odd coupled mode but causes a decrease in Z_o for the even coupled mode.

All available published data is based on quasi-static analyses except in a few cases. Basically, in this study a third dimension, frequency or D/λ, is introduced. Two 3-D plots are given in Figures 20 and 21 to illustrate this point. The x-axis is D/λ, the y axis W/D, and the z-axis

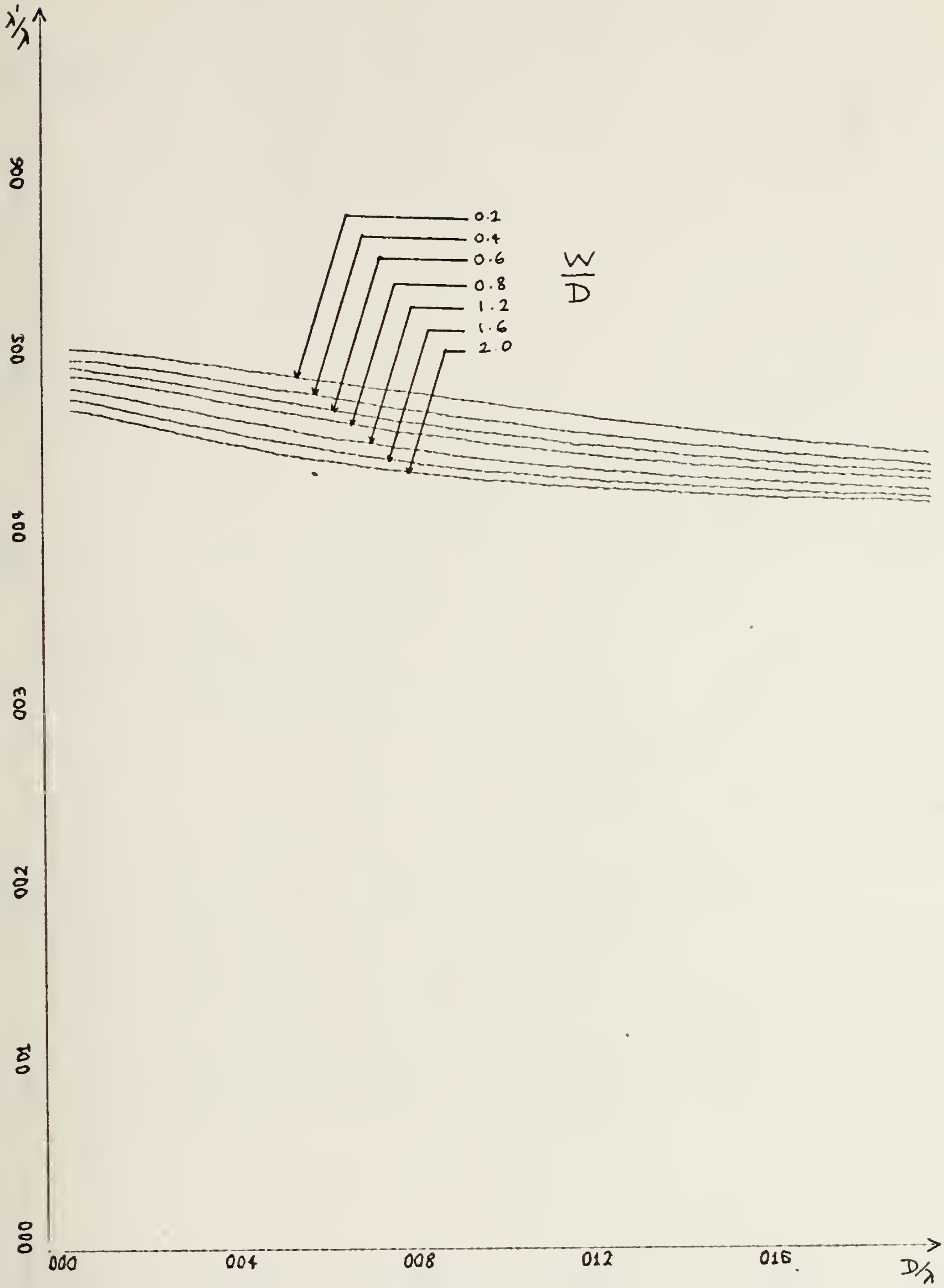

X-SCALE=4.00E-02 UNITS INCH.
Y-SCALE=1.00E-01 UNITS INCH.

Figure 12. Single Strip λ'/λ versus D/λ curves ε_{r_2} = 6.0.

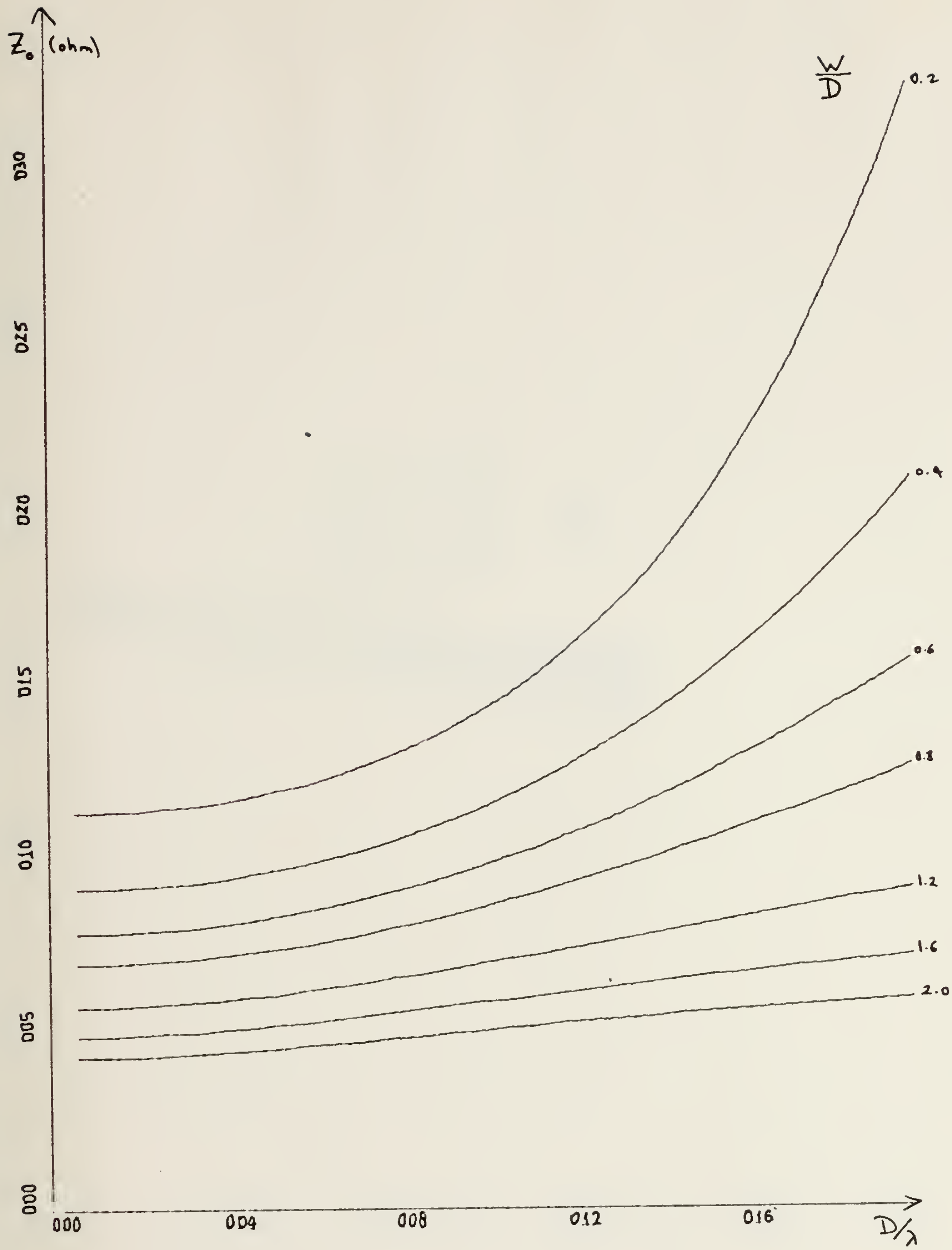

X-SCALE=4.00E-02 UNITS INCH.
Y-SCALE=5.00E+01 UNITS INCH.

Figure 13. Single strip Z_o versus D/λ curves ε_{r_2} = 6.0.

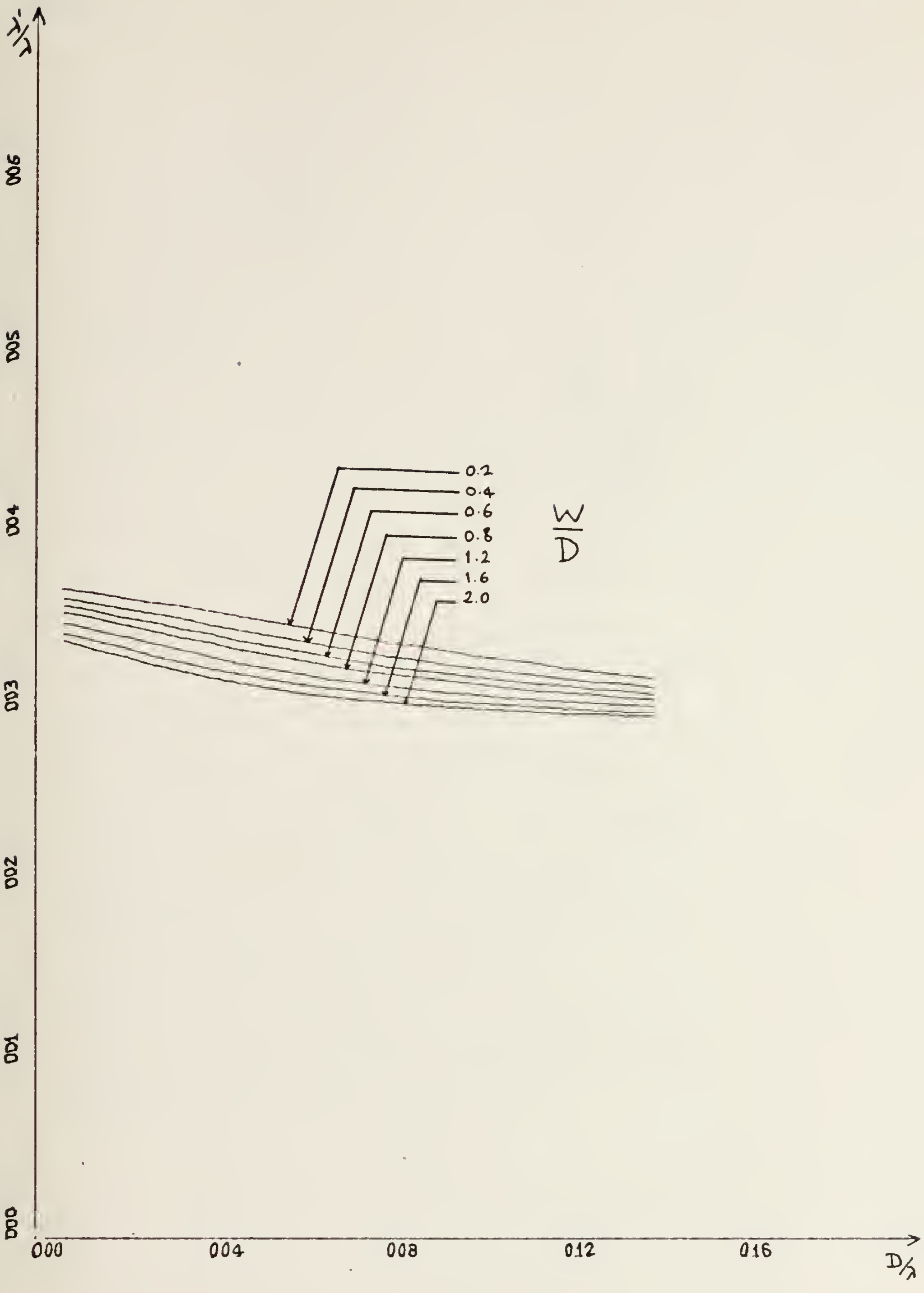

X-SCALE=4.00E-02 UNITS INCH.
Y-SCALE=1.00E-01 UNITS INCH.

Figure 14. Single strip λ'/λ versus D/λ curves $\varepsilon_{r_2} = 12.0$

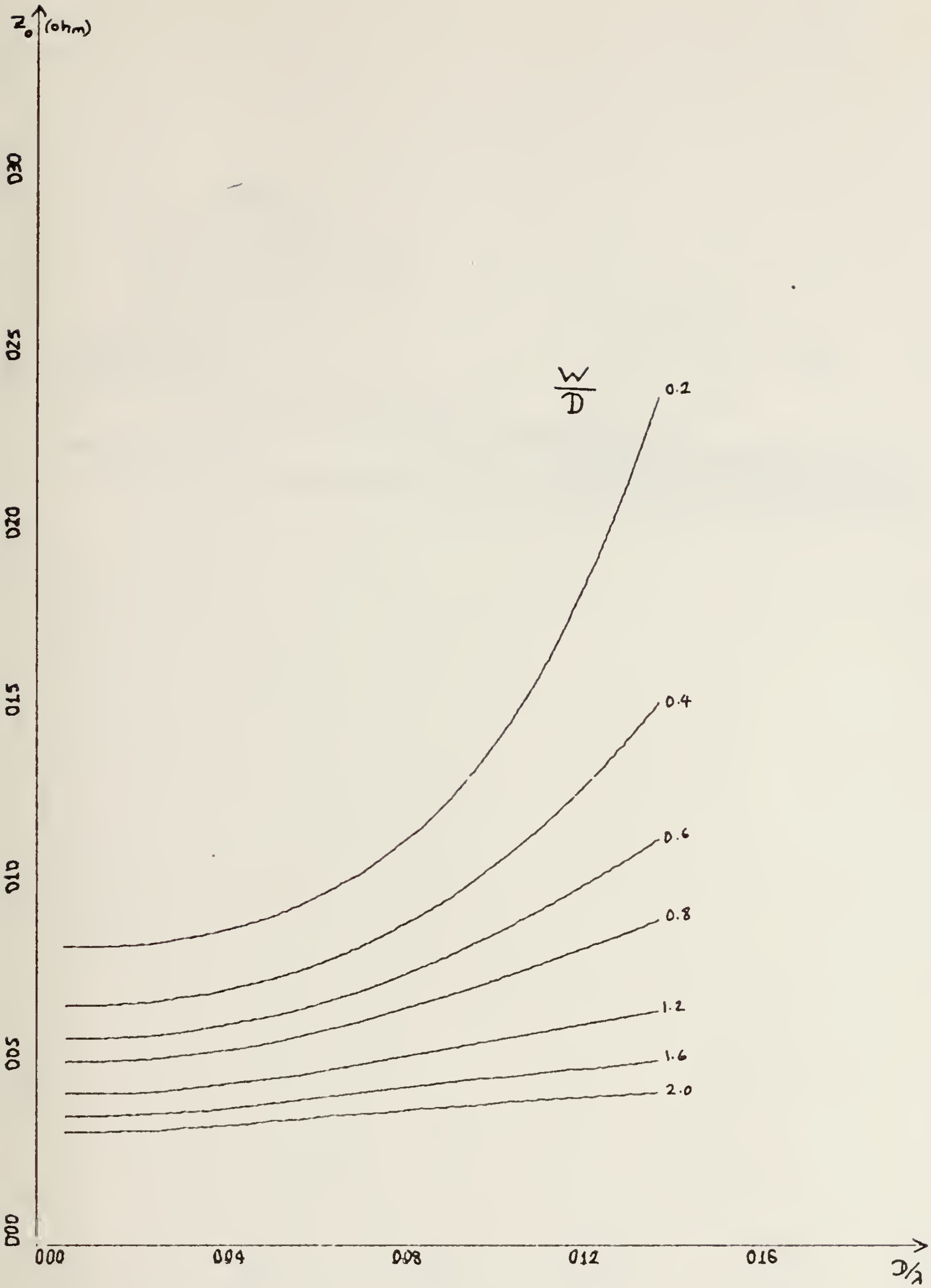

X-SCALE=4.00E-02 UNITS INCH.
Y-SCALE=5.00E+01 UNITS INCH.

Figure 15. Single strip Z_o versus D/λ curves ε_{r_2} = 12.0.

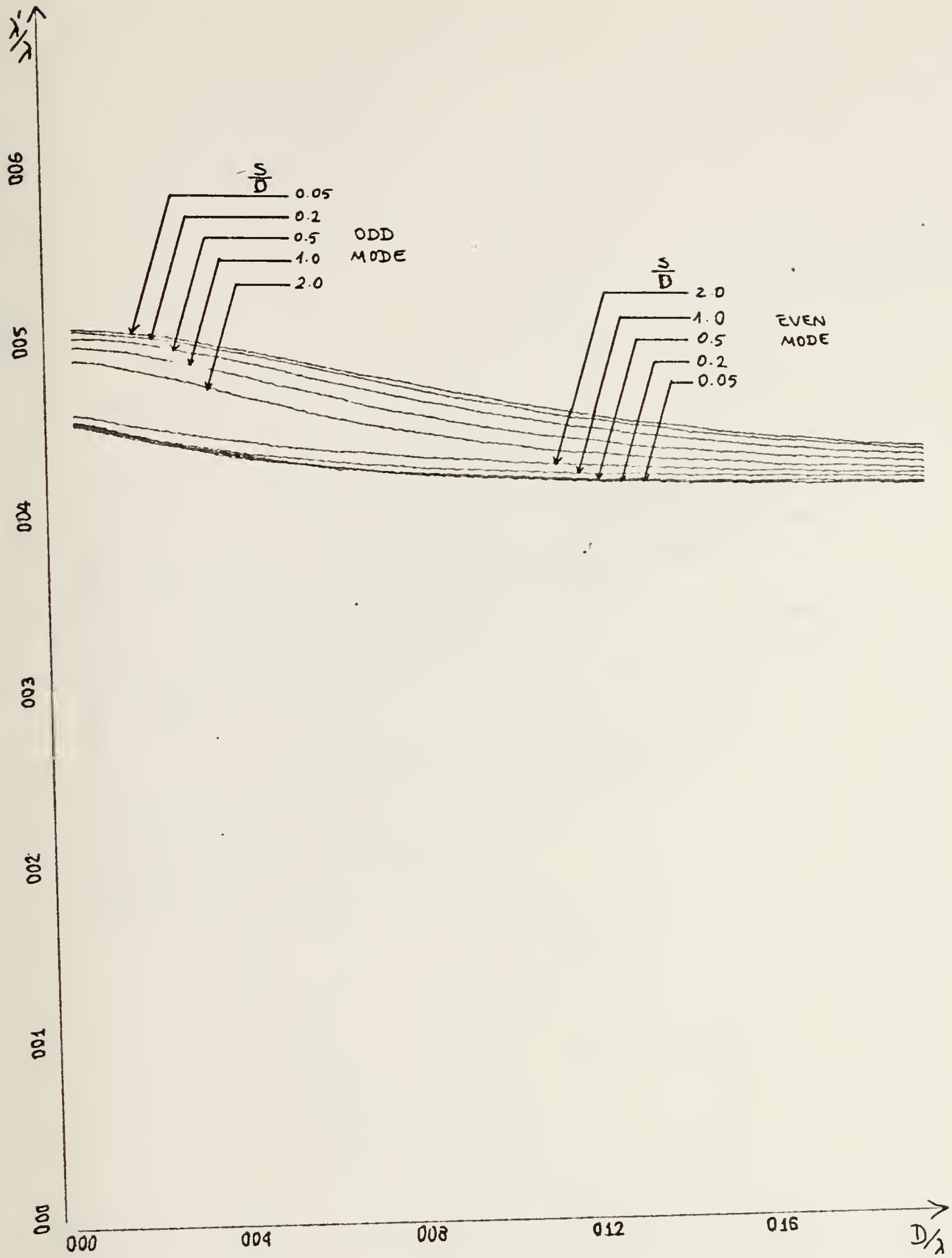

X-SCALE=1.00E-02 UNITS INCH
Y-SCALE=1.00E-01 UNITS INCH

Figure 16. Coupled strip even and odd modes λ'/λ versus D/λ curves ε_{r_2} = 6.0 W/D = 1.54.

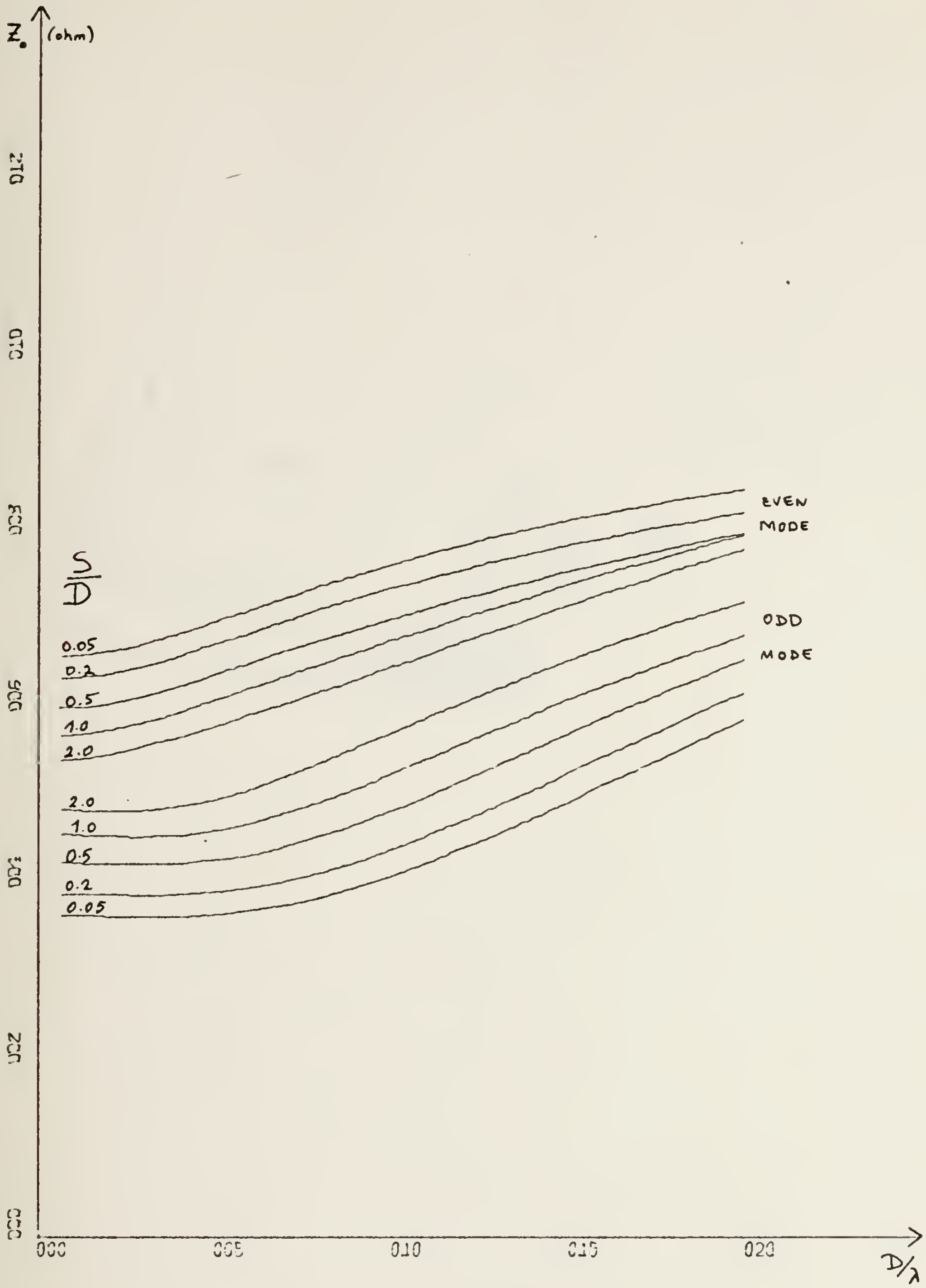

X-SCALE=5.00E-02 UNITS INCH.
Y-SCALE=2.00E+01 UNITS INCH.

Figure 17. Coupled strip even and odd modes Z_o versus D/λ curves $\varepsilon_{r_2} = 6.0$ $W/D = 1.54$.

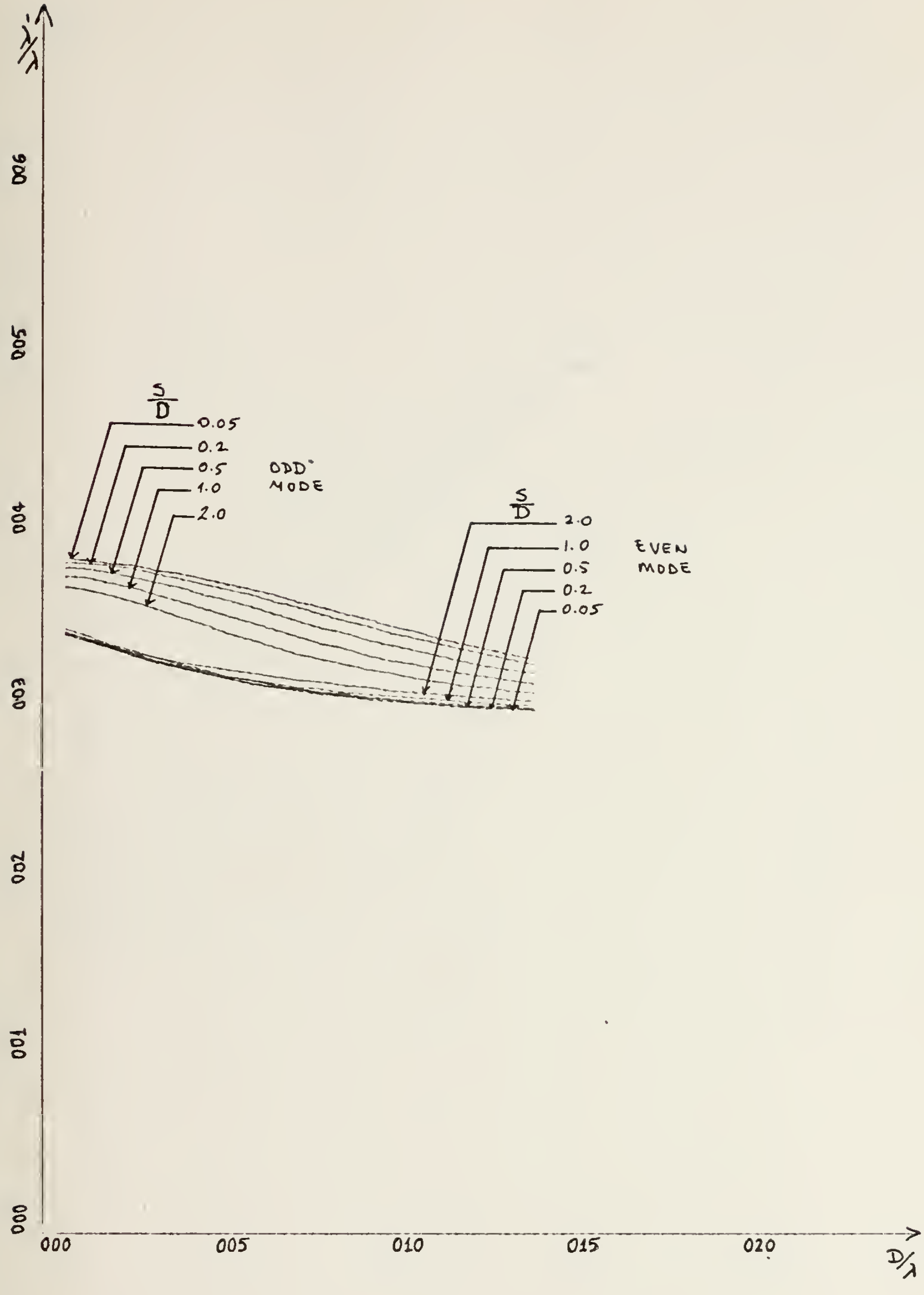

X-SCALE 5.00E-02 UNITS INCH.
Y-SCALE 1.00E-01 UNITS INCH.

Figure 18. Coupled strip even and odd modes λ'/λ versus D/λ curves ε_{r_2} = 12.0 W/D = 0.8.

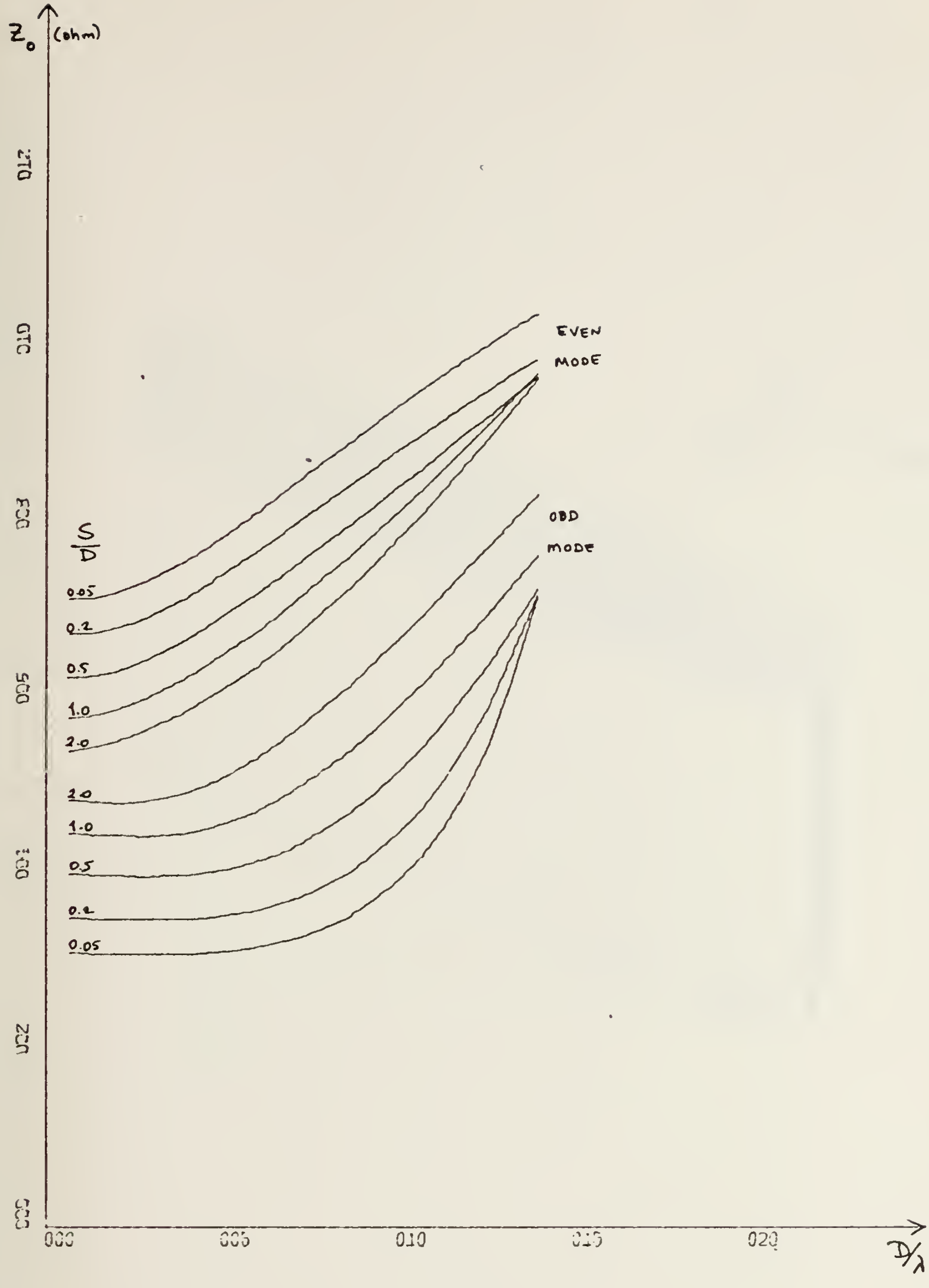

X-SCALE=5.00E-02 UNITS INCH.
Y-SCALE=2.00E+01 UNITS INCH.

Figure 19. Coupled strip even and odd modes Z_o versus D/λ curves ε_{r_2} = 12.0 W/D = 0.8.

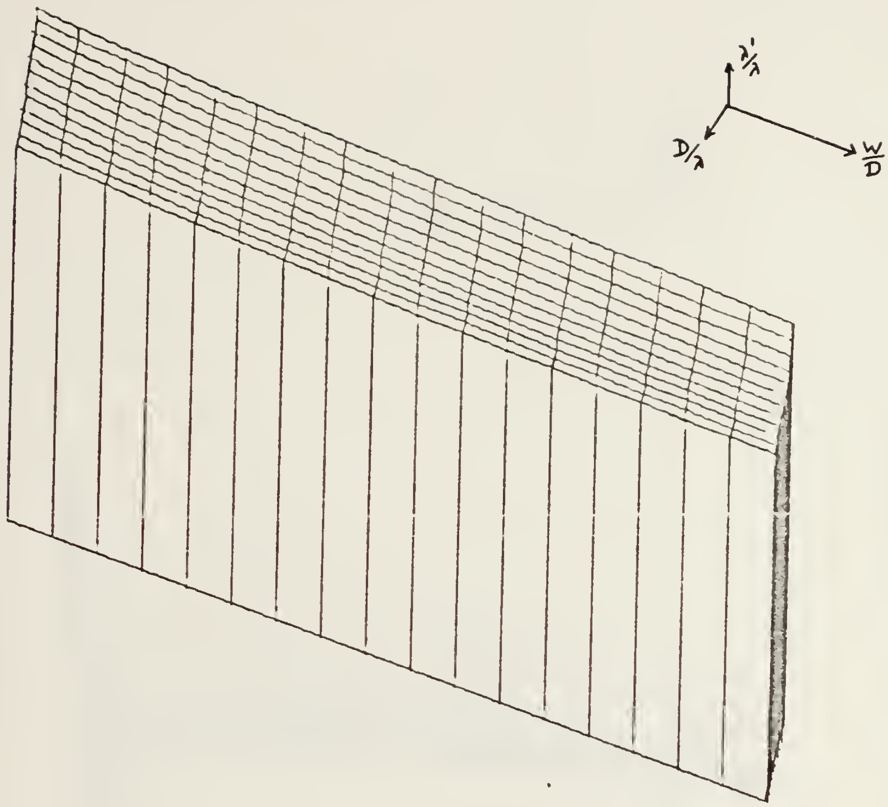

Figure 20. Three dimensional plot λ'/λ, W/D, D/λ single strip.

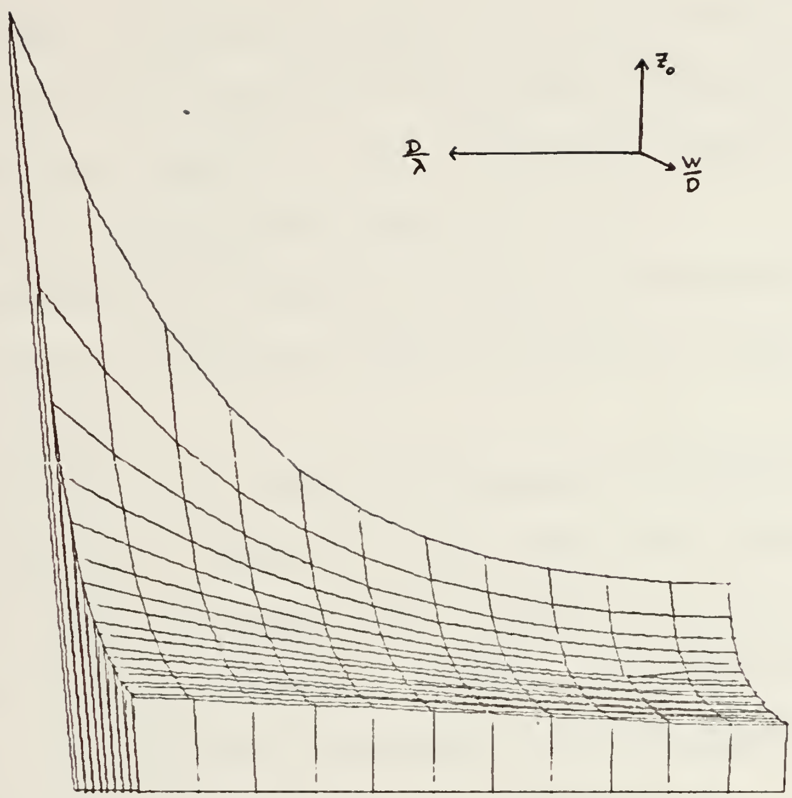

Figure 21. Three dimensional plot Z_0, W/D, D/λ single strip.

λ'/λ and Z_o respectively. One can find the λ'/λ versus W/D and Z_o versus W/D surfaces already plotted in different references, i.e. [Ref. 10] but only for zero frequency.

This newly added dimension makes it possible to find data for a specific frequency in addition to a certain geometry.

In Table I the values found for characteristic impedance with two different methods in Reference 3 and generated from this study are compared. This comparison reflects the agreement in the low frequency range.

Also some of the tabulated data in Reference 11 is compared with data obtained from this study in Table II for coupled strips.

One of the few studies of frequency dependence was by Haddad [Ref. 9]. Table III shows data taken from Haddad's work and from this study which clearly indicates the agreement also for low frequency ranges. Although Haddad's analysis was frequency dependent, the data presented by him was restricted to relatively low frequencies.

Finally three sample computer output pages are given in Tables IV, V and VI.

Although the wavelength and characteristic impedance of microstrips on dielectric substrate depend only upon D/λ, the normalized frequency, this is not true for ferrite substrates. Since the computer program will calculate results for either case it is necessary to provide actual dimensions, D, W, S etc. as inputs. Where both frequency and D/λ are

TABLE I. Characteristic Impedances of Microstrip Transmission Lines Single Strip.

$\varepsilon_{r_2} = 6.0$

W/D	Z_o^*(ohm)	$Z_o^\dagger$(ohm)	Z_o^s(ohm)
0.1	135.455	134.352	137.64
0.2	113.272	112.255	115.41
0.4	91.172	89.909	93.25
0.7	73.613	71.995	73.53
1.0	62.713	60.970	64.45
2.0	43.149	41.510	44.15
4.0	27.301	26.027	27.23
10.0	13.341	12.485	12.58

$\varepsilon_{r_2} = 16.0$

W/D	Z_o^*(ohm)	$Z_o^\dagger$(ohm)	Z_o^s(ohm)
0.1	85.9659	87.762	87.70
0.2	71.6954	73.025	73.43
0.4	57.4999	58.110	59.20
0.7	46.2344	46.217	47.83
1.0	39.2512	38.948	40.72
2.0	26.7555	26.248	27.73
4.0	16.7210	16.300	16.96
10.0	8.0385	7.807	7.77

* Characteristic impedance obtained by method of moment [Ref. 3]

† Characteristic impedance obtained by conformal mapping [Ref. 3]

s Characteristic impedance obtained by spectral domain method in this study.

Table II. Effective Dielectric Constant and Characteristic Impedance for Coupled Strips.

	EVEN MODE				ODD MODE			
W/H	$\varepsilon^*_{r_{eff}}$	$\varepsilon^\dagger_{r_{eff}}$	Z^*_o(ohm)	$Z^\dagger_o$(ohm)	$\varepsilon^*_{r_{eff}}$	$\varepsilon^\dagger_{r_{eff}}$	Z^*_o(ohm)	$Z^\dagger_o$(ohm)
0.1	6.25	6.25	152.98	153.13	5.50	5.51	64.92	65.29
0.3	6.54	6.54	111.07	113.17	5.52	5.54	45.97	49.02
0.5	6.77	6.76	90.40	92.77	5.56	5.59	39.15	43.43
0.7	6.96	6.95	76.88	79.29	5.61	5.66	35.09	39.95
0.9	7.13	7.12	67.13	69.45	5.67	5.73	32.19	37.29
1.1	7.28	7.28	59.69	61.85	5.73	5.82	29.92	35.06
1.3	7.41	7.42	53.80	55.79	5.79	5.90	28.05	33.12
1.5	7.53	7.55	49.0	50.81	5.85	6.00	26.46	31.83
1.7	7.63	7.67	45.02	46.66	5.92	6.09	25.07	29.80
1.9	7.73	7.77	41.66	43.13	5.99	6.19	23.85	28.36

* Weiss Results

† Spectral Domain Transform method used in this study.

Table III. Frequency Dependence of Single and Coupled Microstrip.

	SINGLE W/D = 1.0		COUPLED (EVEN MODE) W/D = 1.0 S/D = 0.4		COUPLED (ODD MODE) W/D = 1.0 S/D = 0.4	
	$\varepsilon^*_{r_{eff}}$	$\varepsilon^\dagger_{r_{eff}}$	$\varepsilon^*_{r_{eff}}$	$\varepsilon^\dagger_{r_{eff}}$	$\varepsilon^*_{r_{eff}}$	$\varepsilon^\dagger_{r_{eff}}$
1GHZ	6.78	6.78	7.39	7.43	5.84	5.85
2GHZ	7.05	6.98	7.8	7.72	5.87	5.94
	Z^*_o	$Z^\dagger_o$	Z^*_o	$Z^\dagger_o$	Z^*_o	$Z^\dagger_o$
1GHZ	48.5Ω	50.88Ω	61.8Ω	62.24Ω	36.2Ω	39.31Ω
2GHZ	50.0Ω	51.22Ω	63.0Ω	62.8 Ω	36.2Ω	39.18Ω

* Haddad results

† Spectral Domain Transform method used in this study.

Table IV. Sample Computer Output for Single Strip.

W = 1mm D = 2mm ε_{r_2} = 12 W/D = 0.5

FREQUENCY	D/LAMBDA	L/LPR	LPR/L	CH IMPEDANCE
1.000 GHZ	0.00667	2.75971	0.36236	62.59 OHM
2.000 GHZ	0.01333	2.78140	0.35953	62.70 OHM
3.000 GHZ	0.02000	2.80726	0.35622	63.07 OHM
4.000 GHZ	0.02667	2.83508	0.35272	63.72 OHM
5.000 GHZ	0.03333	2.86373	0.34919	64.68 OHM
6.000 GHZ	0.04000	2.89254	0.34572	65.96 OHM
7.000 GHZ	0.04667	2.92108	0.34234	67.56 OHM
8.000 GHZ	0.05333	2.94907	0.33909	69.51 OHM
9.000 GHZ	0.06000	2.97628	0.33599	71.81 OHM
10.000 GHZ	0.06667	3.00258	0.33305	74.47 OHM
11.000 GHZ	0.07333	3.02787	0.33027	77.51 OHM
12.000 GHZ	0.08000	3.05206	0.32765	80.94 OHM
13.000 GHZ	0.08667	3.07512	0.32519	84.77 OHM
14.000 GHZ	0.09333	3.09702	0.32289	89.01 OHM
15.000 GHZ	0.10000	3.11775	0.32074	93.66 OHM
16.000 GHZ	0.10667	3.13733	0.31874	98.73 OHM
17.000 GHZ	0.11333	3.15577	0.31688	104.24 OHM
18.000 GHZ	0.12000	3.17311	0.31515	110.17 OHM
19.000 GHZ	0.12667	3.18939	0.31354	116.52 OHM
20.000 GHZ	0.13333	3.20464	0.31205	123.31 OHM

Table V. Sample Computer Output for Coupled Strip (Odd Mode)

W = 1.6mm D = 2.0mm S = 0.8mm W/D = 0.8 S/D = 0.4 $\varepsilon_{r_2} = 12$

FREQUENCY	D/LAMBDA	L/LPR	LPR/L	CH IMPEDANCE
1.000 GHZ	0.00667	2.61034	0.38309	39.05 OHM
2.000 GHZ	0.01333	2.61858	0.38189	38.97 OHM
3.000 GHZ	0.02000	2.63141	0.38002	38.89 OHM
4.000 GHZ	0.02667	2.64815	0.37762	38.84 OHM
5.000 GHZ	0.03333	2.66821	0.37478	38.87 OHM
6.000 GHZ	0.04000	2.69112	0.37159	39.00 OHM
7.000 GHZ	0.04667	2.71640	0.36813	39.26 OHM
8.000 GHZ	0.05333	2.74366	0.36448	39.69 OHM
9.000 GHZ	0.06000	2.77249	0.36069	40.31 OHM
10.000 GHZ	0.06667	2.80248	0.35683	41.16 OHM
11.000 GHZ	0.07333	2.83325	0.35295	42.26 OHM
12.000 GHZ	0.08000	2.86441	0.34911	43.65 OHM
13.000 GHZ	0.08667	2.89561	0.34535	45.34 OHM
14.000 GHZ	0.09333	2.92649	0.34171	47.37 OHM
15.000 GHZ	0.10000	2.95675	0.33821	49.75 OHM
16.000 GHZ	0.10667	2.98613	0.33488	52.51 OHM
17.000 GHZ	0.11333	3.01442	0.33174	55.67 OHM
18.000 GHZ	0.12000	3.04146	0.32879	59.23 OHM
19.000 GHZ	0.12667	3.06714	0.32604	63.22 OHM
20.000 GHZ	0.13333	3.09139	0.32348	67.65 OHM

Table VI. Sample Computer Output for Coupled Strip (Even Mode)

W=1.6mm D=2.0mm S=0.8mm W/D = 0.8 S/D = 0.4 ε_{r_2} = 12

FREQUENCY	D/LAMBDA	L/LPR	LPR/L	CH IMPEDANCE
1.000 GHZ	0.00667	2.92702	0.34164	64.22 OHM
2.000 GHZ	0.01333	2.96430	0.33735	64.38 OHM
3.000 GHZ	0.02000	3.00492	0.33279	64.92 OHM
4.000 GHZ	0.02667	3.04470	0.32844	65.82 OHM
5.000 GHZ	0.03333	3.08186	0.32448	67.00 OHM
6.000 GHZ	0.04000	3.11570	0.32096	68.42 OHM
7.000 GHZ	0.04667	3.14609	0.31786	70.00 OHM
8.000 GHZ	0.05333	3.17316	0.31514	71.70 OHM
9.000 GHZ	0.06000	3.19719	0.31278	73.49 OHM
10.000 GHZ	0.06667	3.21849	0.31070	75.35 OHM
11.000 GHZ	0.07333	3.23740	0.30889	77.26 OHM
12.000 GHZ	0.08000	3.25422	0.30729	79.20 OHM
13.000 GHZ	0.08667	3.26921	0.30588	81.16 OHM
14.000 GHZ	0.09333	3.28263	0.30463	83.14 OHM
15.000 GHZ	0.10000	3.29467	0.30352	85.13 OHM
16.000 GHZ	0.10667	3.30552	0.30252	87.13 OHM
17.000 GHZ	0.11333	3.31533	0.30163	89.14 OHM
18.000 GHZ	0.12000	3.32423	0.30082	91.15 OHM
19.000 GHZ	0.12667	3.33234	0.30009	93.17 OHM
20.000 GHZ	0.13333	3.33975	0.29942	95.18 OHM

shown as printed output the calculation is based on the substrate thickness, D, provided as an input. A width of D = 2mm has been used in the calculations presented here.

VI. CONCLUSIONS

In this thesis a hybrid mode analysis of single and coupled microstrips (of equal width) on dielectric substrate was described. The resulting equations were solved by the method of moments applied in the spectral or (Fourier) transform domain. A computer program was developed to calculate wavelength and characteristic impedance versus frequency. The original results obtained by this method were compared in the low frequency limit with the quasi-static results of several other investigators and were found to be in excellent agreement.

The method was extended to microstrip on ferrite where the propagation constant was calculated using perturbation theory. Numerical evaluation of resulting expressions is again carried out in the spectral domain. A computer program has been developed for this analysis also.

APPENDIX A

AUXILIARY VECTOR POTENTIAL FUNCTIONS

A. MAGNETIC HERTZIAN VECTOR POTENTIAL FUNCTION

Consider a homogeneous, source-free, isotropic region; hence, there is no charge density and

$$\overline{\nabla}\cdot\overline{E} = 0 \tag{A1}$$

From Vector Algebra, it is known that the divergence of a vector is zero if the vector is, in turn, the curl of another vector; therefore, one can state,

$$\overline{\nabla}\cdot\overline{\nabla}\times\overline{\pi}_h = 0 \quad \forall\, \overline{\pi}_h \tag{A2}$$

$$\overline{E} = -j\omega\mu\overline{\nabla}\times\overline{\pi}_h. \tag{A3}$$

For time-varying fields

$$\overline{\nabla}\times\overline{H} = j\omega\varepsilon\ \overline{E} \tag{A4}$$

so applying equation (A3),

$$\begin{aligned}\overline{\nabla}\times\overline{H} &= j\omega\varepsilon(-j\omega\mu\overline{\nabla}\times\overline{\pi}_h)\\ &= k^2\nabla\times\pi_h\\ &= k^2\overline{\nabla}\times(\overline{\pi}_h + k^{-2}\overline{\nabla}\phi)\end{aligned} \tag{A5}$$

$$\overline{H} = k^2\overline{\pi}_h + \overline{\nabla}\phi \tag{A6}$$

where,

$$k^2 = \omega^2\mu\varepsilon.$$

Similarly, for time-varying fields,

$$\overline{\nabla}\times\overline{E} = -j\omega\mu\overline{H} \tag{A7}$$

so, applying equation (A3),

$$\overline{\nabla}x(-j\omega\mu\overline{\nabla}x\overline{\pi}_h) = -j\omega\mu(k^2\overline{\pi}_h + \overline{\nabla}\phi) \tag{A8}$$

$$\overline{\nabla\nabla}\cdot\overline{\pi}_h - \nabla^2\overline{\pi}_h = k^2\overline{\pi}_h + \overline{\nabla}\phi. \tag{A9}$$

Up to this point ϕ has been defined; arbitrarily choose

$$\phi = \overline{\nabla}\cdot\overline{\pi}_h. \tag{A10}$$

Then, equation (A9) becomes,

$$\nabla^2\overline{\pi}_h + k^2\overline{\pi}_h = 0. \tag{A11}$$

Also, it is known that

$$\overline{\nabla}\cdot\overline{B} = \mu\overline{\nabla}\cdot\overline{H} = 0$$

$$\mu\overline{\nabla}\cdot(k^2\overline{\pi}_h + \overline{\nabla}\phi) = 0 \tag{A12}$$

$$k^2\overline{\nabla}\cdot\overline{\pi}_h + \overline{\nabla}\cdot\overline{\nabla}\phi = 0.$$

Summarizing, for TM modes,

$$\overline{E} = -j\omega\mu\overline{\nabla}x\overline{\pi}_h \tag{A13}$$

$$\overline{H} = k^2\overline{\pi}_h + \overline{\nabla\nabla}\cdot\overline{\pi}_h \tag{A14}$$

$$= \overline{\nabla}x\overline{\nabla}x\overline{\pi}_h.$$

Similarly, for TE modes,

$$\overline{H} = j\omega\varepsilon\overline{\nabla}x\overline{\pi}_h \tag{A15}$$

$$\overline{E} = k^2\overline{\pi}_e + \overline{\nabla\nabla}\cdot\overline{\pi}_e \tag{A16}$$

$$= \overline{\nabla}x\overline{\nabla}x\overline{\pi}_e.$$

B. TE AND TM MODES FROM VECTOR POTENTIALS

1. <u>TE Modes</u>

$$\overline{E} = -j\omega\mu\overline{\nabla}x\overline{\pi}^h \tag{A17}$$

$$\overline{H} = k_c^2\overline{\pi}^h + \overline{\nabla}\overline{\nabla}\cdot\overline{\pi}^h$$

$$= \overline{\nabla}x\overline{\nabla}x\overline{\pi}^h \qquad (A18)$$

where $\overline{\pi}^h$ satisfies:

$$\nabla^2\overline{\pi}^h + k_c^2\overline{\pi}^h = 0 \qquad (A19)$$

For TE modes, $E_z = 0$; therefore

$$E_z = -j\omega\mu \left(\frac{\partial\pi_y^h}{\partial x} - \frac{\partial\pi_x^h}{\partial y} \right) \qquad (A20)$$

from where,

$$\pi_x^h = \pi_y^h = 0. \qquad (A21)$$

Let:

$$\overline{\pi}^h = \phi^h e^{-\gamma z}\overline{a}_z \qquad (A22)$$

Then, from equation (A13)

$$\nabla_t^2\phi^h + k_c^2\phi^h = 0 \qquad (A23)$$

where,

$$k_c^2 = \gamma^2 + k^2. \qquad (A24)$$

Summarizing,

$$H_z = k_c^2\phi^h(x,y)e^{\pm\gamma z} \qquad (A25)$$

$$\overline{H}_t = \pm\gamma e^{\pm\gamma z}\nabla_t\phi^h \qquad (A26)$$

$$\overline{E}_t = \pm\frac{j\omega\mu}{\gamma}\ \overline{a}_z x\overline{H}_t \qquad (A27)$$

2. <u>TM Modes</u>

$$\overline{E} = k_c^2\overline{\pi}^e + \overline{\nabla}\overline{\nabla}\cdot\overline{\pi}^e \qquad (A28)$$

$$= \overline{\nabla}x\overline{\nabla}x\overline{\pi}^e$$

$$\overline{H} = j\omega\varepsilon\overline{\nabla}x\overline{\pi}^e \qquad (A29)$$

For TM Modes, $H_z = 0$; therefore

$$\overline{\pi}^e = \phi^e(x,y)e^{-\gamma z}\overline{a}_z \tag{A30}$$

and,

$$\nabla_t^2\phi^e + k_c^2\phi^e = 0 \tag{A31}$$

where,

$$k_c^2 = \gamma^2 + k^2. \tag{A32}$$

Summarizing,

$$E_z = k_c^2\phi^e e^{\pm\gamma z} \tag{A33}$$

$$\overline{E}_t = \pm\gamma\overline{\nabla}_t\phi^e e^{\pm\gamma z} \tag{A34}$$

$$\overline{H}_t = \mp \frac{j\omega\varepsilon}{\gamma}\,\overline{a}_z x\overline{E}_t. \tag{A35}$$

Equations (1) and (2) correspond to equations (A33) and (A25), respectively.

APPENDIX B

TRANSVERSE ELECTRIC AND MAGNETIC FIELDS

Consider Maxwell's point form of Amere's law,

$$\overline{\nabla}\times\overline{H} = j\omega\varepsilon\overline{E} \tag{B1}$$

$$\overline{a}_x\left(\frac{\partial H_z}{\partial y} - \frac{\partial H_y}{\partial z}\right) + \overline{a}_y\left(\frac{\partial H_x}{\partial z} - \frac{\partial H_z}{\partial x}\right) + \overline{a}_z\left(\frac{\partial H_y}{\partial x} - \frac{\partial H_x}{\partial y}\right)$$

$$= j\omega\varepsilon(E_x\overline{a}_x + E_y\overline{a}_y + E_z\overline{a}_z) \tag{B2}$$

from where,

$$\frac{\partial H_z}{\partial y} - \frac{\partial H_y}{\partial z} = j\omega\varepsilon E_x \tag{B3}$$

$$\frac{\partial H_x}{\partial z} - \frac{\partial H_z}{\partial x} = j\omega\varepsilon E_y \tag{B4}$$

$$\frac{\partial H_y}{\partial x} - \frac{\partial H_x}{\partial y} = j\omega\varepsilon E_z \tag{B5}$$

and, due to the z-dependence of the fields, i.e., $e^{\gamma z}$, one can apply

$$\frac{\partial}{\partial z} e^{\gamma z} = \gamma e^{\gamma z} \tag{B6}$$

obtaining from equations (B3) through (B5)

$$\frac{\partial H_z}{\partial y} - \gamma H_y = j\omega\varepsilon E_x \tag{B7}$$

$$\gamma H_x - \frac{\partial H_z}{\partial x} = j\omega\varepsilon E_y \tag{B8}$$

$$\frac{\partial H_y}{\partial x} - \frac{\partial H_z}{\partial y} = j\omega\varepsilon E_z. \tag{B9}$$

Similarly, starting from Maxwell's point form of Lenz' law,

$$\overline{\nabla} x \overline{E} = -j\omega\mu\overline{H} \tag{B10}$$

$$\overline{a}_x \left(\frac{\partial E_z}{\partial y} - \frac{\partial E_y}{\partial z} \right) + \overline{a}_y \left(\frac{\partial E_x}{\partial z} - \frac{\partial E_z}{\partial x} \right) + \overline{a}_z \left(\frac{\partial E_y}{\partial x} - \frac{\partial E_x}{\partial y} \right)$$

$$= -j\omega\mu(H_x\overline{a}_x + H_y\overline{a}_y + H_z\overline{a}_z) \tag{B11}$$

from where,

$$\frac{\partial E_z}{\partial y} - \gamma E_y = -j\omega\mu H_x \tag{B12}$$

$$\gamma E_x - \frac{\partial E_z}{x} = -j\omega\mu H_y \tag{B13}$$

$$\frac{\partial E_y}{\partial x} - \frac{\partial E_x}{\partial y} = -j\omega\mu H_z \tag{B14}$$

Substituting the value of E_x from equation (B13) into equation (B7), one obtains

$$\frac{\partial H_z}{\partial y} - \gamma H_y = \frac{j\omega\varepsilon}{\gamma} \left(\frac{\partial E_z}{\partial x} - j\omega\mu H_y \right)$$

$$H_y(\gamma^2+\omega^2\mu\varepsilon) = \gamma \frac{\partial H_z}{\partial y} - j\omega\varepsilon \frac{\partial E_z}{\partial x} \tag{B15}$$

$$H_y = \frac{1}{k_c^2} \left(\gamma \frac{\partial H_z}{\partial y} - j\omega\varepsilon\frac{\partial E_z}{\partial x} \right).$$

Similarly, substituting the values of E_y from equation (B12) into equation (B8), of H_x from equation (B8) into equation (B12) and of H_y from equation (B7) into equation (B13), one obtains

- For H_x,

$$\gamma H_x - \frac{\partial H_z}{\partial x} = j\omega\varepsilon \frac{1}{\gamma} \left(\frac{\partial E_z}{\partial y} + j\omega\mu H_x \right)$$

$$H_x(\gamma^2+\omega^2\mu\varepsilon) = \gamma \frac{\partial H_z}{\partial x} + j\omega\varepsilon \frac{\partial E_z}{\partial y} \tag{B16}$$

$$H_x = \frac{1}{k_c^2} \left(\frac{\partial H_z}{\partial x} + j\omega\varepsilon \frac{\partial E_z}{\partial y} \right).$$

- For E_y,

$$\frac{\partial E_z}{\partial y} - \gamma E_y = -j\omega\mu \frac{1}{\gamma} \left(\frac{\partial H_z}{\partial x} + j\omega\varepsilon E_y \right)$$

$$E_y(\gamma^2+\omega^2\mu\varepsilon) = \gamma \frac{\partial E_z}{\partial y} + j\omega\mu \frac{\partial H_z}{\partial x} \tag{B17}$$

$$E_y = \frac{1}{k_c^2} \left(\frac{\partial E_z}{\partial y} + j\omega\mu \frac{\partial H_z}{\partial x} \right).$$

- For E_x,

$$\gamma^2 E_x - \gamma \frac{\partial E_z}{\partial x} = -j\omega\mu \left(\frac{\partial H_z}{\partial y} - j\omega\varepsilon E_x \right)$$

$$E_x(\gamma^2+\omega^2\mu\varepsilon) = \gamma \frac{\partial E_z}{\partial x} - j\omega\mu \frac{\partial H_z}{\partial y} \tag{B18}$$

$$E_x = \frac{1}{k_c^2} \left(\frac{\partial E_z}{\partial x} - j\omega\mu \frac{\partial H_z}{\partial y} \right).$$

Summarizing,

$$E_x = \frac{1}{k_c^2} \left(\gamma \frac{\partial E_z}{\partial x} - j\omega\mu \frac{\partial H_z}{\partial y} \right) \tag{B19}$$

$$E_y = \frac{1}{k_c^2} \left(\gamma \frac{\partial E_z}{\partial y} + j\omega\mu \frac{\partial H_z}{\partial x} \right) \tag{B20}$$

$$H_x = \frac{1}{k_c^2} \left(\gamma \frac{\partial H_z}{\partial x} + j\omega\varepsilon \frac{\partial E_z}{\partial y} \right) \tag{B21}$$

$$H_y = \frac{1}{k_c^2} \left(\gamma \frac{\partial H_z}{\partial y} - j\omega\varepsilon \frac{\partial E_z}{\partial x} \right). \tag{B22}$$

Equations (B3) through (B6) correspond to equations (B19) through (B22), respectively.

APPENDIX C

AVERAGE POWER EXPRESSION IN REGION 2

(TRIGONOMETRIC CASE)

Electric and Magnetic field potential functions and derivatives with respect to y become

$$\Phi_2^e(\alpha,y) = jB_T^e(\alpha)\,\mathrm{Sin}\gamma_2''y \tag{C1}$$

$$\Phi_2^h(\alpha,y) = C_T^h(\alpha)\,\mathrm{Cos}\gamma_2''y \tag{C2}$$

$$\frac{\partial\Phi_2^e(\alpha,y)}{\partial y} = j\gamma_2''B_T^e(\alpha)\,\mathrm{Cos}\gamma_2''y \tag{C3}$$

$$\frac{\partial\Phi_2^h(\alpha,y)}{\partial y} = -\gamma_2''C_T(\alpha)\,\mathrm{Sin}\gamma_2''y. \tag{C4}$$

Substituting into (115)

$$P_{2AVE_T} = \frac{1}{4\pi}\,\mathrm{Re}\Bigg\{\iint_{\substack{\text{TRIG}\\\text{REGION}}}\int_0^D\Bigg([-\alpha^2\beta\omega\varepsilon_2|B_T^e(\alpha)\,\mathrm{Sin}\gamma_2''y|-\omega\beta\mu_2$$

$$|-\gamma_2''C_T^h(\alpha)\,\mathrm{Sin}\gamma_2''y|^2-\omega\beta\varepsilon_2|j\gamma_2''B_T^e(\alpha)\,\mathrm{Cos}\gamma_2''y|^2-\alpha^2\omega\mu_2\beta|C_T^h(\alpha)\,\mathrm{Cos}\gamma_2''y|^2]$$

$$+j\alpha k_2^2[(C_T^h(\alpha)\,\mathrm{Cos}\gamma_2''y)(-j\gamma_2''B_T^{e*}(\alpha)\,\mathrm{Cos}\gamma_2''y) + (-jB_T^{e*}(\alpha)\,\mathrm{Sin}\gamma_2''y)$$

$$(-\gamma_2''C_T^h(\alpha)\,\mathrm{Sin}\gamma_2''y)] - j\alpha\beta^2[(jB_T^e(\alpha)\,\mathrm{Sin}\gamma_2''y)(-\gamma_2''C_T^{h*}(\alpha)\,\mathrm{Sin}\gamma_2''y)$$

$$+ (C_T^{h*}(\alpha)\,\mathrm{Cos}\gamma_2''y)(j\gamma_2''B_T^e(\alpha)\,\mathrm{Cos}\gamma_2''y)]\Bigg)dy\,d\alpha\Bigg\} \tag{C5}$$

Then,

$$P_{2_{AVE_T}} = \frac{1}{4\pi}\,\mathrm{Re}\Bigg\{\iint_{\substack{\text{TRIG}\\\text{REGION}}}\int_0^D \mathrm{Sin}^2\gamma_2''y\,dy\,[-\alpha^2\beta\omega\varepsilon_2|B_T^e(\alpha)|^2$$

$$-\omega\beta\mu\gamma_2''^2|C_T^h(\alpha)|^2-\alpha^2k_2^2\gamma_2''C_T^h(\alpha)B_T^{e*}(\alpha)-\alpha\beta^2\gamma_2''B_T^e(\alpha)C_T^{h*}(\alpha)]\,d\alpha$$

$$+\iint_{\substack{\text{TRIG}\\\text{REGION}}}\int_0^D \mathrm{Cos}^2\gamma_2''y\,dy\,[-\ \omega\beta\varepsilon_2\gamma_2''^2|B_T^e(\alpha)|^2-\alpha^2\omega\mu_2\beta|C_T^h(\alpha)|^2$$

$$+\ \alpha k_2^2\gamma_2''C_T^h(\alpha)B_T^{e*}(\alpha)\ +\ \alpha\beta^2\gamma_2''B_T^e(\alpha)C_T^{h*}(\alpha)]\,d\alpha\Bigg\}. \tag{C6}$$

Also the integration with respect to y in Region 2 may be accomplished analytically as indicated below:

$$\int_0^D \mathrm{Sin}^2\gamma_2''y\,dy = \frac{2\gamma_2''D\ -\ \mathrm{Sin}2\gamma_2''D}{4\gamma_2''} \tag{C7}$$

$$\int_0^D \mathrm{Cos}^2\gamma_2''y\,dy = \frac{2\gamma_2''D\ +\ \mathrm{Sin}2\gamma_2''D}{4\gamma_2''} \tag{C8}$$

By substituting (C7) and (C8) in (C6) and rearranging one can easily obtain

$$P_{2_{AVE_T}} = -\ \frac{1}{16\pi}\,\mathrm{Re}\Bigg\{\int_{\substack{\text{TRIG}\\\text{REGION}}} (2\gamma_2''D\ -\ \mathrm{Sin}2\gamma_2''D)[\frac{\alpha^2\beta\omega\varepsilon_2}{\gamma_2''}\ |B_T^e(\alpha)|^2$$

$$+\ \beta\omega\mu_2\gamma_2''|C_T^h(\alpha)|^2+\alpha k_2^2C_T^h(\alpha)B_T^{e*}(\alpha)\ +\ \alpha\beta^2B_T^e(\alpha)C_T^{h*}(\alpha)]\,d\alpha\ +$$

$$\int_{\substack{\text{TRIG}\\\text{REGION}}} (2\gamma_2''D\ +\ \mathrm{Sin}2\gamma_2''D)[\frac{\alpha^2\beta\omega\mu_2}{\gamma_2''}\ \ |C_T^h(\alpha)|^2\ +\ \beta\omega\varepsilon_2\gamma_2''|B_T^e(\alpha)|^2$$

$$\alpha\beta^2B_T^e(\alpha)C_1^{*h}(\alpha)\ -\ k_2^2C_T^h(\alpha)B_T^{e*}(\alpha)]\,d\alpha\Bigg\}. \tag{C9}$$

The final equation (C9) corresponds to equation (130).

APPENDIX D

```
C       THIS PROGRAM IS DEVELCPED TO CALCULATE THE EFFECTIVE
C       WAVELENGTH AND CHARACTERISTIC IMPEDANCE OF SINGLE OR
C       CCUPLED  MICROSTRIP ON A DIELECTRIC OR FERRITE
C       SUBSTRATE.IF THE SUBSTRATE IS FERRITE LOSS PER
C       WAVELENGTH IN DB AND NORMALIZED PHASE SHIFT ARE
C       ALSO CALCULATED.
C       PROGRAM ACCEPTS FOLLOWING INPUT  DATA
C       FIRST CARD -IDENTIFICATION  DIGITS FORMAT(I3)
C       THIS THREE DIGIT INTEGER SUPPLIES NECCESARY
C       INFORMATION TO THE PROGRAM
C       FIRST  DIGIT   1  MEANS DIELECTRIC SUBSTRATE
C       FIRST  DIGIT   2  MEANS FERRITE    SUBSTRATE
C       SECOND DIGIT   1  MEANS SINGLE     STRIP
C       SECOND DIGIT   2  MEANS  COUPLED   STRIP
C       THIRD DIGIT    1  MEANS  EVEN  MODE
C       THIRD DIGIT    2  MEANS  ODD   MODE
C       THIRD  DIGIT  IS  USED ONLY FOR COUPLED
C       STRIP WHEN SECOND DIGIT IS EQUAL TO 2.ALL
C       OTHER TIMES SHOULD BE SET TO ZERO.
C       EXAMPLES
C       110   SINGLE STRIP DIELECTRIC SUBSTRATE
C       211   COUPLED STRIP EVEN MODE ON FERRITE SUBSTRATE
C       SECOND  CARD -EPR1,MR1,MR2 FORMAT(3F10.5)
C       EPR1 IS THE RELATIVE DIELECTRIC PERMITTIVITY REGION 1
C       MR1  IS THE RELATIVE MAGNETIC PERMEABILITY REGION 1
C       MR2  IS THE RELATIVE MAGNETIC PERMEABILITY REGION 2
C       THIRD CARD- DD, WW1,SS    FORMAT(3F10.5)
C       DD- THICKNESS OF THE SUBSTRATE  IN MILLIMETERS
C       WW1-WIDTH OF THE STRIPS         IN MILLIMETERS
C       SS- SEPERATION BETWEEN STRIPS   IN MILLIMETERS
C       FOURTH CARD- FREQGH  FORMAT(F10.5)
C       FREQGH IS THE INITIAL FREQUENCY (GIGAHERTZ)
C       FIFTH CARD- IN FORMAT(I2)
C       IN-INDEX NUMBER OF RELATIVE DIELECTRIC
C       PERMITTIVITIES TO BE READ IN NEXT CARDS
C       SIXTH AND FOLLOWING CARDS CONTAIN  VALUES OF
C       EPR2 IN REGION TWO ONE FOR EACH  CARD (F10.5)
C
C       THE METHOD USED IN FINDING THE EFFECTIVE
C       WAVELENGTH IN THE STRUCTURE IS BASED ON A ROOT
C       SEARCHING ALGORITHM  SPECIFICALLY DEVELOPED
C       FOR  THIS  STUDY.
C       PROGRAM DEVELOPED  BY LT(JG)  AHMET M. TUFEKCIOGLU
C       TURKISH NAVY
C       THESIS ADVISOR -PROF. JEFFREY B. KNORR  PH.D.
C       NAVAL POSTGRADUATE  SCHOOL MONTEREY CALIFORNIA
C       SEPTEMBER  1974
C
C       ALL VARIABLES  ARE DOUBLE PRECISION  REAL*8
C
        IMPLICIT REAL*8(A-H,K-Z)
        DIMENSION FYA(80), FYB(80), FYC(80), FYD(80), TRRA(2)
        DIMENSION YX(80), YY(80), YZ(80), YC(80), YF(80)
        DIMENSION TS1(2), TS2(2), TS3(2), TST(4)
        COMMON /FER/ PNS,IFSW
        COMMON /ZEYNEP/ S,IEO
        COMMON /ADA/ D,WOVD,WW
        COMMON /AT/ TA,TB,TC,TD,PI,BETAD,TE2,EPR2,IFLG
        COMMON /EMRE/ TE,TF,FA2,FA3,FB1,FB2,FB9,FC1,FC2,FD1
        EXTERNAL GZR,GZIM
        DATA TS1/'DIELECTR',' FERRITE'/
        DATA TS2/'  SINGLE',' COUPLED'/
        DATA TS3/'   EVEN ','   ODD  '/
        READ (5,18) IDF,ISC,IEO
        READ (5,19) EPR1,MR1,MR2
        READ (5,19) DD,WW1,SS
        READ (5,20) FREQGH
        READ (5,21) IN
```

```
      PI = 3.14159265358979D0
      PISQ = PI**2
      EPS = 0.1**1
      D = DD*1.E-3
      S = SS*1.E-3
      WW = WW1*1.E-3
      WCVD = WW/D
      FREQDD = FREQGH
C     SETTING LOWER AND UPPER LIMITS OF INTEGRATICN
      BCB = -2.*PI/WW
      BBB = -BCB
C
      DO 17 IK=1,IN
      READ (5,20) EPR2
      KAK = DSQRT(EPR2)
      FREQGH = FREQDD
      WRITE (6,22) TS2(ISC),TS1(IDF)
      WRITE (6,25) WOVD
      IF (ISC.EQ.1) GO TO 1
      WRITE (6,26) WW1,SS,TS3(IEO)
      GO TO 2
    1 WRITE (6,23) WW1
    2 WRITE (6,24) EPR2,MR2,DD
      IFRS = IDINT(.15/(KAK*D))
C     MAXIMUM FREQUENCY  RANGE  TO BE COVERED
C     IN  GIGAHERTZ  TO AVOID  HIGHER ORDER MODES
      IF (IFRS.GT.50) IFRS=50
C
      DO 14 IS=1,IFRS
C     IFLG  IS A FLAG WHEN EQUALS TO 1  CHARACTERISTIC
C     IMPEDANCE  CALCULATED. IFSW IS THE FERRITE  SWITCH
C     WHEN IS EQUAL TO 1 FERRITE SUBSTRATE  RELATED
C     CALCULATIONS  ARE DONE
      IFLG = 0
      IFSW = 0
      FREQ = FREQGH*1.E9
      LAM = 3.E8/FREQ
C
      DOVL = D/LAM
C     ROOT FINDING ROUTINE STARTS
C     USTL=UPPER LIMIT FOR  L/LPR
C     ALTL=LOWER LIMIT  FOR  L/LPR
      USTL = KAK-.01
      IF (IS-2) 3,4,4
    3 ALTL = (USTL+1.)/2.
      GO TO 5
    4 ALTL = LOVLPR
    5 LOVLPR = USTL
      ALTL1 = ALTL
      IA = 1
C     INTERMEDIATE  ALGEBRAIC  STEPS
    6 BETAD = 2.0*PI*DOVL*LOVLPR
      TA1 = 240.0*PISQ*DOVL
      TA = TA1*MR2
      TB1 = DOVL/60.0
      TB = TB1*EPR2
      TC = TA1*MR1
      TD = TB1*EPR1
C
      DOVLSQ = DOVL**2
      TE1 = LOVLPR**2
      TE2 = 4.0*PISQ*DOVLSQ
      TE = -TE2*(TE1-1.0)
      TF = TE2*(EPR2-TE1)
      FA2 = TE/TC
      FA3 = TF/TA
      FB1 = BETAD/TC
      FB2 = BETAD/TA
      FB9 = TE/TF
      FD1 = BETAD/TE
      FC1 = TD/TE
      FC2 = TB/TF
```

```
C     VALUES OF ALFA  WHERE  GAMMA 2  SWITCHES
C     REAL TO IMAGINARY
      ALF = DSQRT(TF/D**2)
      ALFN = -ALF
C     EVALUATION OF  INTEGRAL
      CALL DQG24 (BCB,ALFN,GZR,Y1)
      CALL DQG24 (ALFN,ALF,GZIM,Y2)
      CALL DQG24 (ALF,BBB,GZR,Y3)
      GZ = Y1+Y2+Y3
      IF (DABS(GZ).LT.EPS) GO TO 11
      IF (IA.NE.1) GO TO 7
      IA = 0
      LOVLPR = ALTL
      GZ1 = GZ
      GO TO 6
    7 IF (DABS(GZ1-GZ).GT.DABS(GZ1)) GO TO 9
      IF (ALTL.NE.ALTL1) GO TO 8
      ALTL = ALTL+0.001
      GO TO 10
    8 USTL = ALTL
      ALTL = (ALTL1+USTL)/2.
      LOVLPR = ALTL
      GZ1 = GZ
      GO TO 6
    9 ALTL1 = ALTL
   10 ALTL = (USTL+ALTL)/2.
      LOVLPR = ALTL
      GO TO 6
   11 YX(IS) = DOVL
      YY(IS) = 1./LOVLPR
      YZ(IS) = LOVLPR
      YF(IS) = FREQGH
      IFLG = 1
C     EVALUATION OF INTEGRAL  FOR CHARACTERISTIC IMPEDANCE.
      CALL DQG24 (BCB,ALFN,GZR,C1)
      CALL DQG24 (ALFN,ALF,GZIM,C2)
      CALL DQG24 (ALF,BBB,GZR,C3)
      CHIMP = (C1+C2+C3)*(1./(8.*PI))*D*2.0
      IF (ISC.EQ.2) CHIMP=CHIMP/2.D0
      YC(IS) = CHIMP
      IF (IDF.NE.2) GO TO 13
C     FERRITE CALCULATIONS STARTS.
C     SET OF PARAMETERS  USED  FOR  SPECIFIC CASE.
      HZERO = 6.0D0
      WZERO = 2.8D0*HZERO
      WZERSQ = WZERO**2
      WALFA = 0.105D0
      WALFSQ = WALFA**2
      WM = 3.36D0
      WMSQ = WM**2
      FERWSQ = (2.*PI*FREQGH)**2
      FERDEN = (WZERSQ-FERWSQ-WALFSQ)**2+4.*WZERSQ*WALFSQ
      XKIPRI = (WM*WZERO*(WZERSQ-FERWSQ+WALFSQ))/FERDEN
      XKIDPR = (WM*WALFA*(WZERSQ+FERWSQ+WALFSQ))/FERDEN
      IFSW = 1
C     INTEGRATION  LIMITS DOUBLED FOR FERRITE PART.
      BAB = 2.*BCB
      BUB = -BAB
C     PNS  IS POSITIVE NEGATIVE SWITCH  FOR +Z AND -Z
C     DIRECTION TRAVELING FIELDS.
      PNS = -1.0D0
C
      DO 12 IXX=1,2
C     EVALUATION OF  INTEGRAL
      CALL DQG24 (BAB,ALFN,GZR,FER1)
      CALL DQG24 (ALFN,ALF,GZIM,FER2)
      CALL DQG24 (ALF,BUB,GZR,FER3)
      TRRA(IXX) = FER1+FER2+FER3
      PNS = PNS**2
   12 CONTINUE
C
      MRMO = 4.D-7*PI
```

```
      SABIT  = (FREQ*D*MRMO)/(4.*CHIMP)
      FYA(IS) = DABS(XKIPRI*TRRA(1)*SABIT)
      FYB(IS) = DABS(XKIPRI*TRRA(2)*SABIT)
      FYC(IS) = DABS(XKIDPR*TRRA(1)*SABIT)
      FYD(IS) = DABS(XKIDPR*TRRA(2)*SABIT)
      BETTA = BETAD/D
      FYA(IS) = (BETTA+FYA(IS))/BETTA
      FYB(IS) = (BETTA+FYB(IS))/BETTA
      FYC(IS) = 8.686*2.*PI*FYC(IS)/(BETTA*FYA(IS))
      FYD(IS) = 8.686*2.*PI*FYD(IS)/(BETTA*FYA(IS))
   13 FREQGH = FREQGH+1.0D0
   14 CONTINUE
C
      WRITE (6,27)
      WRITE (6,28)
C
      DO 15 ITR=1,IFRS
   15 WRITE (6,29) YF(ITR),YX(ITR),YZ(ITR),YY(ITR),YC(ITR)
C
      IF (IDF.NE.2) GO TO 17
      WRITE (6,30)
C
      DO 16 IH=1,IFRS
   16 WRITE (6,31) YF(IH),FYA(IH),FYB(IH),FYC(IH),FYD(IH)
C
   17 CONTINUE
C
      STOP
C
   18 FORMAT (3I1)
   19 FORMAT (3F10.5)
   20 FORMAT (F10.5)
   21 FORMAT (I2)
   22 FORMAT ('1',//55X,'MICROSTRIP ANALYSIS'//55X,A8,2X,
     1 'STRIP'//55X,A8,2X,'SUBSTRATE'/)
   23 FORMAT ('0',55X,'WIDTH OF STRIP=',F5.2)
   24 FORMAT ('0',55X,'EPR2=',F5.2,2X,'MR2=',F5.2//56X,
     1 'THICKNESS D=',F4.1,2X,'MM'/)
   25 FORMAT ('0',60X,13(1H*)/2(61X,1H*,11X,1H*/),61X,1H*,
     1'W/D=',F4.1,3X,
     2  1H*/2(61X,1H*,11X,1H*/),61X,13(1H*)///)
   26 FORMAT ('0',55X,'WIDTH OF STRIP=',F4.1,2X,'MM'//
     1 56X,'SEPERATION',F4.1,2X,'MM'//55X,A8,2X,'MODE')
   27 FORMAT ('0',32X,'FREQUENCY ',2X,' D/LAMBDA ',5X,
     1'L/LPR',6X,'LPR/L',5X,'CH IMPEDANCE')
   28 FORMAT (' ',30X,5(2X,10(1H_))//)
   29 FORMAT ('0',32X,F6.3,1X,'GHZ',3(2X,F10.5),2X,
     1 F6.2,1X,'OHM'/)
   30 FORMAT ('0',8X,'FREQUENCY',8X,'BF-/BPR ',10X,
     1 'BF+/BPR',10X,'2*PI*8.868*DELALFA/B **NEG AND POS')
   31 FORMAT ('0',3X,F10.3,4(4X,F15.6))
      END
```

```
      REAL FUNCTIONGZR*8(ALFA)
C     ROUTINE DEFINES THE  POLYNOMIAL FOR HYPEBOLIC CASE
      IMPLICIT REAL*8(A-H,K-Z)
      COMMCN /FER/ PNS,IFSW
      COMMON /ADA/ D,WOVD,WW
      COMMON /AT/ TA,TB,TC,TD,PI,BETAD,TE2,EPR2,IFLG
      COMMON /EMRE/ TE,TF,FA2,FA3,FB1,FB2,FB9,FC1,FC2,FD1
      ALFAD = ALFA*D
      TG1 = ALFAD**2
      TG = TG1-TE
      VG = DSQRT(TG)
      BB = FB1*ALFAD/VG
      BC = FC1*ALFAD
      TH = TG1-TF
      VH = DSQRT(TH)
      FA1 = 1./DTANH(VH)
      BA = FA1*FB2*ALFAD/VH
      FFF1 = -(FA2/VG+FA3*FA1/VH)
      FFF2 = BB+BA
      FFF3 = -FFF2
      FFF4 = BC*(BB+BA*FB9)-(FC1*VG+FC2*FA1*VH)
      DENOM = FFF1*FFF4-FFF2*FFF3
      GG4 = -FFF1/DENOM
      GG2 = FFF2/DENOM
      CALL TRAN (ALFA,ALFAD,GX)
      IF (IFLG.EC.1) GO TO 1
      GZR = GG4*GX
      RETURN
    1 RCAA = GG4/TE
      RCAA1 = ALFAD*FD1*GG4
      RCAB = (1./(TC*VG))*(GG2-RCAA1)
      RRA = GX*RCAA**2
      RRB = GX*RCAB**2
      RCA = RCAA*RCAB*GX
      RCAC = GG4/(TF*DSINH(VH))
      RCAD = 1./(TA*VH*DSINH(VH))
      RCAE = -GG2+RCAA1*FB9
      RCB = RCAC*RCAD*RCAE*GX
      RRC = GX*RCAC**2
      RRD = GX*(RCAD*RCAE)**2
      P1B = ((TG1+TG)/VG)*(TD*RRA+TC*RRB)*BETAD
      P1C = 2.*ALFAD*(BETAD**2+TE2)*RCA
      P1INT = P1B+P1C
      RKA1 = DSINH(2.*VH)
      RKA = RKA1-(2.*VH)
      RKB = TG1*BETAD*TB*RRC/VH
      RKC = BETAD*TA*VH*RRD
      TAVTB = TE2*EPR2
      RKD = ALFAD*((TAVTB)+BETAD**2)*RCB
      RKE = RKB+RKC-RKD
      RKG = RKA1+(2.*VH)
      RKH = TG1*BETAD*TA*RRD/VH
      RKI = BETAD*TB*VH*RRC
      RKK = (TAVTB+BETAD**2)*ALFAD*RCB
      P2INT = RKA*RKE+RKG*(RKH+RKI-RKK)
      IF (IFSW.EQ.1) GO TO 2
      GZR = P1INT+P2INT*0.5
      RETURN
    2 FERAR = RKA/(2.*VH)
      FERB = (-TG1*BETAD**2+TF**2)*RRD
      FERC = PNS*TB*BETAD*ALFAD*VH*2.0*RCB
      FERD = TH*RRC*TB**2
      GZR = FERAR*(FERB+FERC-FERD)
      RETURN
      END
```

```
      REAL FUNCTIONGZIM*8(ALFA)
      IMPLICIT REAL*8(A-H,K-Z)
      COMMON /FER/ PNS,IFSW
      COMMON /AT/ TA,TB,TC,TD,PI,BETAD,TE2,EPR2,IFLG
      COMMON /ADA/ D,WCVD,WW
      COMMON /EMRE/ TE,TF,FA2,FA3,FB1,FB2,FB9,FC1,FC2,FD1
      ALFAD = ALFA*D
      TG1 = ALFAD**2
      TG = TG1-TE
      VG = DSQRT(TG)
      BB = FB1*ALFAD/VG
      BC = FD1*ALFAD
      TH = -TG1+TF
      VH = DSQRT(TH)
      FA1 = DCOTAN(VH)
      BA = FA1*FB2*ALFAD/VH
      FFF1 = -(FA2/VG-FA3*FA1/VH)
      FFF2 = BB-BA
      FFF3 = -FFF2
      FFF4 = BC*(BB-BA*FB9)-(FC1*VG+FC2*FA1*VH)
      DENOM = FFF1*FFF4-FFF2*FFF3
      GG4 = -FFF1/DENOM
      GG2 = FFF2/DENOM
      CALL TRAN (ALFA,ALFAD,GX)
      IF (IFLG.EQ.1) GO TO 1
      GZIM = GG4*GX
      RETURN
    1 RCAA = GG4/TE
      RCAA1 = ALFAD*FD1*GG4
      RCAB = (1./(TC*VG))*(GG2-RCAA1)
      RRA = GX*RCAA**2
      RRB = GX*RCAB**2
      RCA = RCAA*RCAB*GX
      RCAC = GG4/(TF*DSIN(VH))
      RCAD = 1./(TA*VH*DSIN(VH))
      RCAE = GG2-RCAA1*FB9
      RCB = RCAC*RCAD*RCAE*GX
      RRC = GX*RCAC**2
      RRD = GX*(RCAD*RCAE)**2
      P1B = ((TG1+TG)/VG)*(TD*RRA+TC*RRB)*BETAD
      P1C = 2.*ALFAD*(BETAD**2+TE2)*RCA
      P1INT = P1B+P1C
      RKA1 = DSIN(2.*VH)
      RKA = 2.*VH-RKA1
      RKB = TG1*BETAD*TB*RRC/VH
      RKC = BETAD*TA*VH*RRD
      TAVTB = TE2*EPR2
      RKD = ALFAD*((TAVTB)+BETAD**2)*RCB
      RKE = RKB+RKC+RKD
      RKG = RKA1+(2.*VH)
      RKH = TG1*BETAD*TA*RRD/VH
      RKI = BETAD*TB*VH*RRC
      RKK = (TAVTB+BETAD**2)*ALFAD*RCB
      P2INT = RKA*RKE+RKG*(RKH+RKI-RKK)
      IF (IFSW.EQ.1) GO TO 2
      GZIM = P1INT+P2INT*0.5
      RETURN
    2 FERAI = (RKA1+2.*VH)/(2.*VH)
      FERB = (-TG1*BETAD**2+TF**2)*RRD
      FERC = PNS*TB*BETAD*ALFAD*VH*2.0*RCB
      FERD = TH*RRC*TB**2
      GZIM = FERAI*(FERB+FERC-FERD)
      RETURN
      END
```

```
      SUBROUTINE TRAN (ALTR,ALFD,GXTR)
      IMPLICIT REAL*8(A-H,K-Z)
      COMMON /ZEYNEP/ S,IEO
      COMMON /ADA/ D,WOVD,WW
      CB = ALFD*WOVD*0.5
      GX1 = ((1./CB)*(DSIN(CB)))**2
      IF (IEO.EQ.0) GO TO 2
      CD = ALTR*(S+WW)*0.5
      IF (IEO.EQ.2) GO TO 1
      GX1 = GX1*(2.*DCOS(CD))**2
      GO TO 2
    1 GX1 = GX1*(2.*DSIN(CD))**2
    2 GXTR = GX1
      RETURN
      END
```

LIST OF REFERENCES

1. R. E. Collin, Field Theory of Guided Waves, pp. 179-180, McGraw-Hill Book Co., New York, 1960.

2. E. Denlinger, "A Frequency Dependent Solution for Microstrip Transmission Lines," IEEE Trans Microwave Theory and Techniques Vol. MTT-19, pp.30-39, January 1971.

3. A. Farrar and A. T. Adams, "Characteristic Impedance of Microstrip by the Method of Moments," IEEE Trans Microwave Theory and Techniques Vol. MTT-7, January 1970, pp. 65-66.

4. R. Harrington, "Matrix Methods for Field Problems," IEEE Proceedings, Vol. 55, pp. 136-138, February 1967.

5. J. Helszajn, Principles of Microwave Engineering, pp. 53-65 and pp. 117-130, Wiley, 1969.

6. T. Itoh and R. Mittra, "Spectral-Domain Approach for Calculating the Dispersion Characteristics of Microstrip Lines," IEEE Trans Microwave Theory and Techniques, Vol. MMT-21, pp. 496-499, July 1973.

7. J. B. Knorr, "Perturbation of Wave Guide Material," Unpublished Class Notes, Naval Postgraduate School, Monterey, California.

8. J. B. Knorr, "Analysis of Single and Coupled Microstrip," Unpublished Class Notes, Naval Postgraduate School, Monterey, California.

9. M. Krage and G. Haddad, "Frequency Dependent Characteristic of Microstrip Transmission Lines," IEEE Trans Microwave Theory and Techniques, Vol. MTT-20, pp. 678-688, October 1972.

10. Microwave Engineering Handbook Vol 1., p. 132-137, Artech House Inc., 1971.

11. J. Weiss, et. al., "Parameters of Microstrip Transmission Lines and of Coupled Pairs of Microstrip Lines," IEEE Trans Microwave Theory and Techniques, Vol. MTT-16, pp. 1021-1026, December 1968.

INITIAL DISTRIBUTION LIST

		No. Copies
1.	Defense Documentation Center Cameron Station Alexandria, Virginia 22314	2
2.	Library, Code 0212 Naval Postgraduate School Monterey, California 93940	2
3.	Professor Richard W. Adler, Code 52Ab Department of Electrical Engineering Naval Postgraduate School Monterey, California 93940	1
4.	Professor Jeffery B. Knorr, Code 52Ko Department of Electrical Engineering Naval Postgraduate School Monterey, California 93940	2
5.	LT (jg) Ahmet M. Tüfekçioğlu, Turkish Navy Başa Sok.Fırtına Apt. No. 13/21 Levent-Istanbul TURKEY	2
6.	Istanbul Teknik Üniversitesi Elektrik Fakültesi Taskısla, Istanbul, TURKEY	1
7.	Orta Doğu Teknik Üniversitesi Elektrik-Elektronik Fakültesi Ankara, TURKEY	1
8.	Professor Sydney R. Parker, Code 52 Department of Electrical Engineering Naval Postgraduate School Monterey, California 93940	1
9.	Boğaziçi Teknik Üniversitesi Bebek, Istanbul, TURKEY	1

156138
Thesis
T85 Tüfekcioğlu
c.1 Hybrid mode analysis of
microstrip on dielectric
and ferrite substrate.